Global Biogeochemical Cycles

RESEARCH ARTICLE
10.1029/2018GB005909

Vegetation Functional Properties Determine Uncertainty of Simulated Ecosystem Productivity: A Traceability Analysis in the East Asian Monsoon Region

Erqian Cui[1,2], Kun Huang[1,2], Muhammad Altaf Arain[3], Joshua B. Fisher[4], Deborah N. Huntzinger[5], Akihiko Ito[6], Yiqi Luo[7], Atul K. Jain[8], Jiafu Mao[9], Anna M. Michalak[10], Shuli Niu[11,12], Nicholas C. Parazoo[4], Changhui Peng[13,14], Shushi Peng[15], Benjamin Poulter[16], Daniel M. Ricciuto[9], Kevin M. Schaefer[17], Christopher R. Schwalm[5,18], Xiaoying Shi[9], Hanqin Tian[19], Weile Wang[20], Jinsong Wang[11], Yaxing Wei[9], Enrong Yan[1], Liming Yan[1], Ning Zeng[21], Qiuan Zhu[14], and Jianyang Xia[1,2]

[1]Zhejiang Tiantong National Forest Ecosystem Observation and Research Station, Shanghai Key Lab for Urban Ecological Processes and Eco-Restoration, Center for Global Change and Ecological Forecasting, School of Ecological and Environmental Sciences, East China Normal University, Shanghai, China, [2]Institute of Eco-Chongming, Shanghai, China, [3]School of Geography and Earth Sciences and McMaster Centre for Climate Change, McMaster University, Hamilton, Ontario, Canada, [4]Jet Propulsion Laboratory, California Institute of Technology, Pasadena, CA, USA, [5]School of Earth Sciences and Environmental Sustainability, Northern Arizona University, Flagstaff, AZ, USA, [6]National Institute for Environmental Studies, Tsukuba, Japan, [7]Center for Ecosystem Science and Society, Department of Biological Sciences, Northern Arizona University, Flagstaff, AZ, USA, [8]Department of Atmospheric Sciences, University of Illinois at Urbana-Champaign, Urbana, IL, USA, [9]Environmental Sciences Division and Climate Change Science Institute, Oak Ridge National Laboratory, Oak Ridge, TN, USA, [10]Department of Global Ecology, Carnegie Institution for Science, Stanford, CA, USA, [11]Department of Resources and Environment, University of Chinese Academy of Sciences, Beijing, China, [12]Key Laboratory of Ecosystem Network Observation and Modeling, Institute of Geographic Sciences and Natural Resources Research, Chinese Academy of Sciences, Beijing, China, [13]Department of Biology Sciences, Institute of Environment Sciences, University of Quebec at Montreal, Quebec, Canada, [14]Center for Ecological Forecasting and Global Change, College of Forestry, Northwest A&F University, Yangling, China, [15]Sino-French Institute for Earth System Science, College of Urban and Environmental Sciences, Peking University, Beijing, China, [16]Department of Ecology, Montana State University, Bozeman, MT, USA, [17]National Snow and Ice Data Center, Cooperative Institute for Research in Environmental Sciences, University of Colorado Boulder, Boulder, CO, USA, [18]Woods Hole Research Center, Falmouth, MA, USA, [19]International Center for Climate and Global Change Research and School of Forestry and Wildlife Sciences, Auburn University, Auburn, AL, USA, [20]Ames Research Center, National Aeronautics and Space Administration, Moffett Field, CA, USA, [21]Department of Atmospheric and Oceanic Science, University of Maryland, College Park, MD, USA

Abstract Global and regional projections of climate change by Earth system models are limited by their uncertain estimates of terrestrial ecosystem productivity. At the middle to low latitudes, the East Asian monsoon region has higher productivity than forests in Europe-Africa and North America, but its estimate by current generation of terrestrial biosphere models (TBMs) has seldom been systematically evaluated. Here, we developed a traceability framework to evaluate the simulated gross primary productivity (GPP) by 15 TBMs in the East Asian monsoon region. The framework links GPP to net primary productivity, biomass, leaf area and back to GPP via incorporating multiple vegetation functional properties of carbon-use efficiency (CUE), vegetation C turnover time (τ_{veg}), leaf C fraction (F_{leaf}), specific leaf area (SLA), and leaf area index (LAI)-level photosynthesis (P_{LAI}), respectively. We then applied a relative importance algorithm to attribute intermodel variation at each node. The results showed that large intermodel variation in GPP over 1901–2010 were mainly propagated from their different representation of vegetation functional properties. For example, SLA explained 77% of the intermodel difference in leaf area, which contributed 90% to the simulated GPP differences. In addition, the models simulated higher CUE (18.1 ± 21.3%), τ_{veg} (18.2 ± 26.9%), and SLA (27.4±36.5%) than observations, leading to the overestimation of simulated GPP across the East Asian monsoon region. These results suggest the large uncertainty of current TBMs in simulating GPP is largely propagated from their poor representation of the vegetation functional properties and call for a better understanding of the covariations between plant functional properties in terrestrial ecosystems.

Key Points:
- A GPP-traceability framework is established to diagnose the uncertainty sources of modeled GPP
- Large intermodel differences of modeled GPP result from their different representation of vegetation functional properties
- Positive bias in simulated GPP over the East Asian monsoon region could be attributed to the higher simulated CUE and SLA comparing with observations

Supporting Information:
- Supporting Information S1

Correspondence to:
J. Xia,
jyxia@des.ecnu.edu.cn

Citation:
Cui, E., Huang, K., Arain, M. A., Fisher, J. B., Huntzinger, D. N., Ito, A., et al. (2019). Vegetation functional properties determine uncertainty of simulated ecosystem productivity: A traceability analysis in the East Asian monsoon region. *Global Biogeochemical Cycles*, *33*, 668–689. https://doi.org/10.1029/2018GB005909

Received 20 FEB 2018
Accepted 9 MAY 2019
Accepted article online 12 MAY 2019
Published online 7 JUN 2019

1. Introduction

Terrestrial ecosystems, storing up to 4 times more carbon (C) than the atmosphere (Lal, 2004), play a pivotal role in predicting future climate change (Beer et al., 2010; Heimann & Reichstein, 2008; Intergovernmental Panel on Climate Change, 2013). The carbon sequestration function of terrestrial ecosystems is initiated with gross primary productivity (GPP), the total CO_2 uptake by plants via photosynthesis. Tropical and boreal regions, which account for the vast majority of the global forest, have been shown to be important terrestrial C sinks (Bunker et al., 2005; Cox et al., 2013; Pfeifer et al., 2015). The middle- to low-latitude regions are shaped by the subtropical anticyclone and are covered mainly by desert, steppe, and shrub ecosystems. However, the East Asian monsoon region (Figure S1 in the supporting information; Yu et al., 2014), benefits from the interaction of tropical maritime and polar continental air masses (Duan & Wu, 2005), and is typically composed of distinctive evergreen broadleaved forests (Song et al., 2015). According to field observations based on eddy covariance technique, the subtropical forests of the East Asian Monsoon region accounts for 8% of global forests' net ecosystem productivity (NEP; 0.72 $\pm$ 0.08 Pg C/year; Yu et al., 2014). Thus, accurately simulating the dynamics of productivity in this region is crucial for predicting the global land-atmosphere CO_2 exchange and C feedback to climate change from subtropical ecosystems.

In recent decades, terrestrial ecosystems in the East Asian Monsoon region have been strongly shaped by rapid climate changes as well as intense anthropogenic disturbances. Rising temperatures (R. Zhang, 2015) and increased nitrogen deposition (Wang et al., 2017) have been detected in this region. The average summer rainfall (which accounts for more than half of the total annual precipitation) exhibits strong spatial variability, in response to the decadal shifts of East Asian summer monsoon (Zhang et al., 2015). Land-use types in this region have been intensively disturbed or managed by human activities. For instance, most of the evergreen broadleaved forest is gradually being replaced by the secondary communities (Song et al., 2015; Tan et al., 2012), and redistribution of cropland have resulted in significant changes of carbon storage (Tian et al., 2003). These environmental factors may have different impacts on the long-term trend of GPP in the East Asian Monsoon region. Terrestrial biosphere models (TBMs) are proved to be useful tools for evaluating regional ecosystem productivity and its variations in response to environmental changes. It is still unclear, however, to what extent the inter-model GPP variability can be explained by their different response to environmental drivers.

Large uncertainty of modeled GPP has been addressed in numerous studies, based on model intercomparison project (MIP) or model-data synthesis (MDS) project. The uncertainties of modeled GPP by current TBMs include intermodel differences and model ensemble biases. Among them, model ensemble biases result from their poor representation or lack of some key processes related to regional characteristics, for example, agricultural shift cultivation, wildfires, insects, disease disturbance, and impacts of forest age. Large intermodel spread of simulated GPP in the TBMs includes external environmental forcing, model structure, and parameters (Ito et al., 2017; Schaefer et al., 2012; Schwalm et al., 2010; Xia et al., 2017). When multiple TBMs are forced by the same environmental forcing, their differences in model structure and parameters could induce intermodel variation of GPP via two approaches. First, many studies have detected that the model-to-model variation of C cycle largely stems from their different initial conditions. For example, there is sixfold difference in simulated soil C-stock among models in the Coupled Model Intercomparison Project Phase 5 at the initial condition (Exbrayat et al., 2014; Todd-Brown et al., 2014). Thus, intermodel difference of simulated productivity could largely result from their representation of the initial vegetation state. Second, most models simulate an increasing trend of global or regional GPP during the twentieth century (Huntzinger et al., 2017; Ito et al., 2017; Xia et al., 2017), but they vary in their sensitivity to specific environmental factors. Thus, we need to systematically diagnosis which processes or parameters drive the inter-model difference in simulating productivity without (i.e., with initial conditions) and under environmental changes in the East Asian Monsoon region.

A large number of studies have been conducted to assess intermodel differences and model performance on ecosystem productivity (Anav et al., 2013; Ito et al., 2016; Xia et al., 2017; Yao et al., 2017). Most of these studies have revealed a twofold to threefold difference in simulated ecosystem productivity among models. Large model ensemble biases have also been emphasized through the comparison of simulations and observation-based results. Reducing such model uncertainty is difficult, because there are a series of subsequent transmission processes of carbon assimilation. These processes include net primary productivity

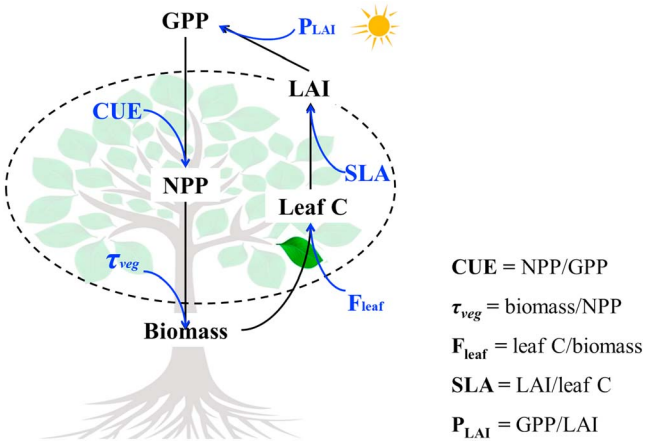

Figure 1. Schematic diagram of the GPP-traceability framework introduced in this study. CUE, C-use efficiency; τ_{veg}, vegetation C turnover time; F_{leaf}, leaf C fraction; SLA, specific leaf area; P_{LAI}, LAI-level photosynthesis. GPP, gross primary productivity; LAI, leaf area index; NPP, net primary productivity.

(NPP), its allocation to various carbon pools, and leaf area dynamics. The cumulative leaf area index (LAI) will in turn affect subsequent canopy level photosynthesis. They are connected in a closed loop by incorporating a set of vegetation functional properties: C-use efficiency (CUE), vegetation C turnover time (τ_{veg}, year), leaf C fraction (F_{leaf}, %), specific leaf area (SLA, cm^2/g), and LAI-level photosynthesis (P_{LAI}, g $C \cdot m^{-2} \cdot year^{-1}$; Figure 1). Most of these subsequent C-accumulation processes and properties are not well quantified by current process-based models (Rogers et al., 2017), and errors in these processes and properties propagate through the GPP-simulation loop and even to the simulation of soil C dynamics. Therefore, a model intercomparison on these connected vegetation processes and their deterministic functional properties are urgently needed to improve the modeling of terrestrial ecosystem productivity.

Here, we examine 15 TBMs participating in the Multi-scale Synthesis and Terrestrial Model Intercomparison Project (MsTMIP) for their ability to estimate GPP in the East Asian Monsoon region during 1901–2010. The model evaluation in our study is based on a traceability framework (Fig. 1). The logic flow of this work is that first we identify the key sources of the intermodel difference in GPP simulation. The effects of initial conditions and environmental changes on intermodel variations in GPP are separately evaluated. Then, modeled GPP is further decomposed into the subsequent C-accumulation processes and associated vegetation functional properties. Their relative contributions in controlling model performance on GPP are also quantified. Second, the key uncertainty processes and vegetation functional properties are evaluated by comparing with available observations and remote sensing data products. The aim of this study is to introduce a GPP-traceability framework to diagnose the sources of intermodel variability in simulated GPP in current TBMs and quantify the major uncertainty sources of modeled GPP for the East Asian Monsoon region.

2. Methods

2.1. Models and Simulation Experiments

The MsTMIP (Huntzinger et al., 2013; Wei et al., 2014b) is a formal model intercomparison effort designed to diagnose the sources of intermodel variability in global-scale models of historic terrestrial carbon cycle dynamics. The TBMs participating in MsTMIP are all driven by the same environmental forcing data sets (Wei et al., 2014a, 2014b) and a standardized spin-up simulation protocol over a 110-year time period from 1901–2010. The simulation protocol includes a series of sensitivity simulations where one time-varying driver is added at a time in order to quantify the sensitivity of simulated carbon cycle changes to four key environmental drivers: climate forcing, land-use change, atmospheric CO_2, and nitrogen deposition (Table S1; Huntzinger et al., 2013). In total, MsTMIP designs five simulation experiments: (1) assume all environmental drivers constant (RG1: initial condition); (2) time-varying historical climate only (SG1); (3) time-varying climate and land-use change (SG2); (4) time-varying climate, land-use changes, and atmospheric CO_2 concentrations (SG3); (5) all drivers are time-varying, including nitrogen deposition rates (BG1). Note that half of the models participating in MsTMIP do not have a coupled C-N cycle and therefore do not submit BG1 simulations. For C-only models, their "best" estimate with all time-varying drivers turned on is SG3. The sensitivity of simulated plant productivity to individual environmental drivers is determined by simulation differencing: climate change = SG1 − RG1, land-use change = SG2 − SG1, atmospheric CO_2 = SG3 − SG2, and nitrogen deposition = BG1 − SG3.

The model outputs used here are taken from the version 1.0 release of MsTMIP yearly retrievals (1901–2010) with a spatial resolution of 0.5° × 0.5° (Huntzinger et al., 2018). The model ensemble includes BIOME-BGC (e.g., Thornton et al., 2002), CLASS-CTEM-N (e.g., Huang et al., 2011), CLM4 (e.g., Mao et al., 2012), CLM4VIC (e.g., Li et al., 2011), DLEM (e.g., Tian et al., 2011), GTEC (e.g., Wang et al., 2011), ISAM (e.g., Jain et al., 2009), LPJ-wsl (e.g., Poulter et al., 2010), ORCHIDEE-LSCE (e.g., Krinner et al., 2005), SiB3 (e.g., Baker et al., 2008), SiBCASA (e.g., Schaefer et al., 2009), TEM6 (e.g., Hayes et al., 2011), TRIPLEX-GHG (e.g., Peng et al., 2013; Zhu et al., 2014), VISIT (e.g., Ito, 2010), and VEGAS2.1 (e.g., Zeng et al., 2005). A

detailed description of variables included in this study is provided in Table S2. Thus, we separated out models with both BG1 and SG3 as the subensembles (7 models) for nitrogen deposition experiment. Likewise, we got the subensembles to conduct the factorial experiments for climate change (14 models), land-use change (13 models), and atmospheric CO_2 (14 models). Note that the vegetation functional properties, such as CUE, τ_{veg}, F_{leaf}, SLA, and P_{LAI}, are not true model parameters (Figure. 1). Here, we used F_{leaf} instead of NPP allocation because of the following reasons: first, almost no MIP has listed the NPP allocation to new growth as standard outputs; second, the limited in situ observations of NPP allocation with its difficult measurements in the natural ecosystems; third, the major contribution of vegetation C turnover time to NPP simulation should be considered in the loop.

2.2. Satellite-Derived GPP and FLUXNET MTE GPP

The modeled GPP over 2000–2010 in the East Asian Monsoon region was evaluated against satellite-derived GPP and FLUXNET measurements with a machine learning technique termed model tree ensemble (hereafter MTE GPP). Satellite-derived GPP was obtained from MODIS on board the National Aeronautics and Space Administration Terra satellite (MOD17A2 GPP: 2000–2010; Running & Zhao, 2015). This product provides a globally consistent and continuous estimation of vegetation productivity at 1-km spatial resolution and 8-day intervals and has been widely used to evaluate modeled GPP (e.g., Anav et al., 2015; Mao et al., 2012). In this study, the MOD17A2 GPP estimates were re-sampled into 0.5° × 0.5° spatial resolution using a nearest neighbor algorithm. The MTE GPP (1982–2010) is based on a global monthly gridded GPP product derived from FLUXNET observations with a machine learning technique termed model tree ensemble (Jung et al., 2011). The MTE GPP product, with a relatively small uncertainty (~120 ± 6 Pg C/year globally), has been extensively used for evaluating model performance in recent years (e.g., Peng et al., 2015; Tjiputra et al., 2013). It should be noted that the existing observation-based GPP datasets also rely upon assumptions and none of them based only on measurements, which may generate some uncertainty for estimating GPP (Anav et al., 2015).

2.3. Satellite-Derived NPP and FLUXNET MTE NPP, Satellite-Derived CUE and LAI Data

Satellite-derived NPP from the MODIS (MOD17A3 NPP) and FLUXNET MTE NPP was used to evaluate the modeled NPP over 2000–2010. The version 55 of this product (Running & Zhao, 2015) includes global NPP at 1 km spatial resolution during 2000–2014. The accuracy of this product has been widely evaluated for a range of regional and global applications (e.g., Rawlins et al., 2015; Xia et al., 2017). In this study, the MOD17A3 NPP was resampled into 0.5° × 0.5° spatial resolution using the nearest neighbor algorithm. Following Smith et al. (2015), the FLUXNET MTE data were converted from GPP to NPP by using a fixed factor 0.5. The CUE was calculated as NPP divided by GPP in the East Asian Monsoon region. The regional distribution of CUE was calculated from MODIS NPP and MODIS GPP at 0.5° spatial resolution.

Two satellite-derived LAI data sets (MOD15A2-LAI and GIMMS3g-LAI) were used to evaluate modeled LAI over 2000–2010 in the East Asian Monsoon region. The MOD15A2-LAI data from the MODIS (MOD15A2 LAI) are an 8-day composite at 1-km spatial resolution (Yan et al., 2016). Defined as the number of equivalent layers of leaves relative to a unit of ground area, satellite-derived LAI is commonly used to calculate surface photosynthesis and evapotranspiration. The GIMMS3g LAI product was produced by Boston University and was derived from the GIMMS Normalized Difference Vegetation Index data set using Feed-Forward Neural Networks (Zhu et al., 2013). The GIMMS3g LAI product provides a global LAI data set at 15-day temporal resolution and 1/12° spatial resolution from 1981 to 2011. We composited the 15-day GIMMS3g LAI data to monthly temporal resolution by averaging the two composites in the same month and resampled them to 0.5° spatial resolution by using the nearest neighbor algorithm (Zhu et al., 2016).

2.4. Data-Oriented Aboveground Biomass Carbon and SLA

The passive microwave-based global aboveground biomass C product (1993–2012) version 1.0 (Liu et al., 2015) was used to evaluate the modeled aboveground biomass over 2000–2010 in the East Asian Monsoon region. The data sources of this product were from the aboveground biomass map for tropical regions by Saatchi and Morel (2011). Saatchi and Morel (2011) used a data fusion model to extrapolate 4,079 in situ field plots and 160,918 lidar-derived AGB values from Latin America, Africa, and Asia to the entire tropical regions. The uncertainty of this benchmark biomass map over Asia is ~30%. Thus, the passive

microwave-based global aboveground biomass C product has relatively higher performance in tropical regions.

Given that plant communities can adjust to the environment via changes in mean trait values, trait-climate relationships are useful to predict spatial distribution of community mean trait values (Swenson & Weiser, 2010). Here an environmental drivers-based SLA data set for subtropical evergreen forests was developed to evaluate the spatial distribution of modeled SLA over 2000–2010 in the East Asian Monsoon region. This SLA dataset is based on the SLA-environment relationship that provided by Verheijen et al. (2013). The inversion process of this SLA product and the associated environmental drivers (Allen et al., 1998; New et al., 2002) are detailed in the supplementary materials. The spatial distribution of evergreen forests in the East Asian Monsoon region is derived from the Land Cover project of the Climate Change Initiative led by the European Space Agency (European Space Agency, 2014). Considering the limited SLA observations for other ecosystems to develop a reliable SLA-environment relationship, the comparison here only for model pixel with subtropical evergreen forests.

2.5. Observation-Based Leaf C Fraction and Vegetation C Turnover Time Data

We used plant C records from datasets developed by Luo et al. (2014) and Zhang et al. (2015) to evaluate the modeled leaf C fraction in the East Asian Monsoon region. The data set consists of plant biomass (root, leaf, and stem biomass) and stand age at 2,048 sites. The observations at different sites were obtained directly from harvest or indirectly from allometric growth equations at ecosystem scale. Leaf C fraction was calculated by F_{leaf} = leaf C/total plant C. The observations of vegetation C turnover time were derived from the database developed by Wang et al. (2017). In order to better match the spatial resolution of modeled results, the observation-based dataset was converted into gridded dataset (pixel size: 0.5°) through the conversion tools ("Point to raster") with "mean" method by using ArcGIS 10.1. The conversion process in this study did not use any environmental covariates. The used method here didn't intend to extrapolate or extend the original data set but just assigned a "mean value" to the grids with more than one values. The grid cell without values is still left blank (Figure S2).

The accuracy of these gridded products has been evaluated by comparing with various field observations. The eddy covariance-based GPP observations in the East Asian monsoon region were listed in Table S4 (Chen et al., 2013; Du et al., 2012; Fang, 2011; Geng, 2011; Guo, 2010; Han, 2008; Hirata et al., 2008; Huang et al., 2011; Kato et al., 2006; Kosugi et al., 2005; Kwon et al., 2010; Lei & Yang, 2010a; Lei & Yang, 2010b; Ono et al., 2013; Saigusa et al., 2005; Saito et al., 2006; Saitoh et al., 2010; Shimoda et al., 2005; Sun, 2012; Takanashi et al., 2005; Tan et al., 2011; Wang et al., 2012; Wu et al., 2010; Yan, 2009; Yu et al., 2013; Zha, 2007; Zhang, 2010; Zhang et al., 2010; Zhao, 2011; Zhu, 2005). The SLA observations were collected from 12 typical subtropical evergreen forests (Guo et al., 2015; Iida et al., 2014; Kröber et al., 2012; Le et al., 2015; Luo et al., 2011; Wang et al., 2012; Xu et al., 2016; Yin et al., 2018). The R^2, root-mean-square error were used to assess the accuracy of gridded products (Tables S3–S6 and Figures S3–S6). In summary, these global products perform well over the East Asian monsoon region ($R^2 = 0.51 - 0.70$).

2.6. The Global Forest Age Data Set

The global forest age data set was used to test the age-dependent leaf biomass fraction distribution in current models. This dataset describes the age distributions of plant functional types (PFT) on a 0.5° grid during 2000–2010 (Poulter et al., 2018). Each grid cell contains information on the fraction of each PFT within an age class. The grid cells with >50% fraction of forest cover were extracted in this study, and the average forest age of each grid cell was calculated by weighting stand age from different PFTs.

2.7. Analytical Methods

To identify the major uncertainty source of modeled ecosystem productivity in the East Asian monsoon region, we first derived the different metrics for each model in each grid over 1901–2010 and then analyzed their contributions to intermodel difference. The final attributions were calculated by averaging the values of contributors at the pixel level. The relative importance analysis was conducted with the "relaimpo" package in R (R Development Core Team, 2011), which is based on variance decomposition for multiple linear regression models (Grömping, 2007). The relaimpo package provides six different methods for analyzing relative importance of each variable in linear regression. We chose one of the most computer intensive and common-used method named 'Lindeman-Merenda-Gold (LMG)'. The LMG method averages the

sequential sum of squares for all possible orders of terms to estimate the percentage of the variance from each term (Lindeman et al., 1980). This method has been widely used in ecological studies for quantifying the relative importance of various factors (Fernández-martínez et al., 2014; Musavi et al., 2017; Xia et al., 2015).

We evaluated performance ("best" estimates from BG1 or SG3) of the TBMs in simulating the key carbon processes using Taylor diagrams (Taylor, 2001). The standard deviation (SD) ratio is an alternative measure of the magnitudes of spatial variation, and correlation coefficient presents the spatial pattern similarity of modeled and satellite-derived/data-oriented carbon processes. An ideal model should have a SD ratio of 1.0 and a correlation coefficient of 1.0.

3. Results

3.1. Temporal and Spatial Variability of Modeled GPP

Even with consistent environmental drivers and simulation protocol, there is a huge intermodel difference in simulated GPP over the East Asian Monsoon region, which significantly larger than the globally averaged twofold to threefold discrepancy (Schwalm et al., 2015). The estimated mean annual GPP of this region during 1901–2010 was 1280 ± 422 g C·m^{-2}·year^{-1}, ranging from 201 ± 13 g C·m^{-2}·year^{-1} in CLASS to 1996 ± 111 g C·m^{-2}·year^{-1} in CLM4 (Figure 2a). The ensemble mean GPP is higher over the southwestern region and lower in the grass-covered northern part. Interannual variability of modeled GPP is rather small before 1980 (the average annual growth rate is 1.55 g C·m^{-2}·year^{-2}), but a significant increase during 1981–2010 with an average annual growth rate of 3.33 g C·m^{-2}·year^{-2}. The spatial pattern of model spread (represented as SD) is similar to the distribution of GPP. Regions with greater model disagreement in GPP were typically composed of subtropical evergreen forest and cropland, especially in southeastern China (Figure 2b). Despite the large spatial difference, the models agreed well in the seasonal pattern of monthly GPP. The large spread in annual GPP among models was mainly attributed to the inconsistency of simulated GPP in summer, with an approximately twofold greater difference in summer than other seasons.

Based on outputs from simulation experiments, the relative contributions of initial conditions (RG1) and environmental impacts (BG1-RG1 for C-N cycle models or SG3-RG1 for C-only models) to the intermodel variation in GPP were successfully separated. As shown in Figure 3, large intermodel differences existed in the responses of GPP to environmental changes, ranging from −11 g C·m^{-2}·year^{-1} in ISAM to 344 g C·m^{-2}·year^{-1} in SIB3, with most models indicating a positive environmental impact on GPP, which increases with time. Modeled GPP derived from initial conditions varies from 170 g C·m^{-2}·year^{-1} (CLASS) to 1,853 g C·m^{-2}·year^{-1} (CLM4), a range that is approximately fourfold of the intermodel variation attributable to environmental impacts. Therefore, the intermodel variation in initial conditions is the primary driver of differences in modeled GPP (with the relative contributions of initial conditions and environmental impacts are 90.8% and 9.2%, respectively). The result from C-only models (Figure 3b) was consistent with that of coupled C-N models (Figure 3a). However, the C-only models had a much smaller spread than C-N models, implying that the incorporation of C-N coupling module enlarged model uncertainty (Du et al., 2018). To better understand the intermodel differences of modeled GPP over the East Asian Monsoon region, we further separately identified the uncertainty sources underlying in initial conditions and environmental impacts.

3.2. Intermodel Variation of Initial Conditions

Based on MsTMIP outputs under initial conditions with constant environmental drivers (RG1), we assessed the intermodel difference in modeled key C processes derived from model structure and parameters. The intermodel variability in key C processes was represented by the coefficient of variation of model simulations (CV: CV = 100% × SD/mean). Here mean and SD values were calculated for mean annual outputs among different models for each pixel. The final results were calculated by averaging the values at the pixel level. As shown in Figure 4a, the modeled LAI and SLA showed the highest CV (53% and 50%, respectively), followed by plant biomass (46%), F_{leaf} (38%), NPP (37%), and GPP (35%). Large intermodel difference in modeled GPP propagated through the closed loop to NPP and biomass, finally condensed to a small range when incorporated into leaf dry matter. But the intermodel difference was further amplified by the extremely different representation of SLA among models.

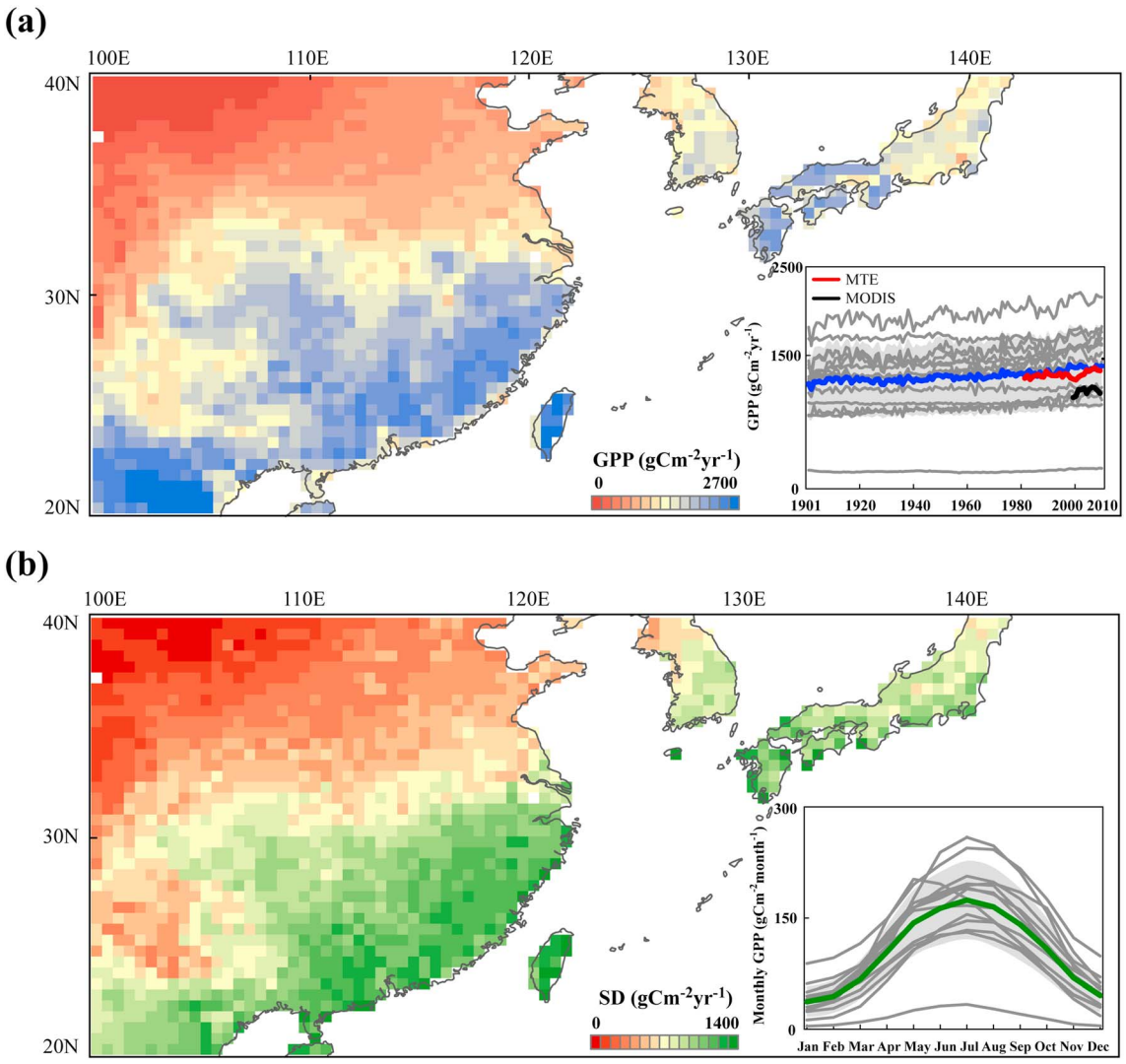

Figure 2. Spatial distributions of (a) multimodel mean GPP and (b) SD of modeled GPP in the East Asian monsoon region deriving from Multi-scale Synthesis and Terrestrial Model Intercomparison Project models. In the insert panel of (a), yearly averaged GPP between 1901 and 2010 from models; in the insert panel of (b), monthly dynamics of GPP from models. The gray lines of insert panels are results from individual models, and the shaded areas are the calculated SD among models. The bold blue line, green line, red line and black line in insert panels are respectively average yearly GPP, average monthly GPP among models, MTE GPP and MODIS GPP. SD, standard deviation.

We then identified the relative importance of the uncertainty sources in modeled key C processes (Figure 4b). The intermodel differences in NPP can be decomposed into that of GPP and CUE. According to the results of variance decomposition, the intermodel variation of simulated NPP is dominated by GPP (~72%) while the relative importance of CUE is only 26%. The lower contribution of τ_{veg} indicated that variation of simulated biomass C mainly resulted from modeled NPP. In addition, intermodel variability of leaf C is largely determined by F_{leaf} (~81%). Considering the higher consistency of modeled leaf C, the differences among modeled LAI were derived from the parameterization of SLA (~77%). Furthermore, the inter-model difference in annual GPP was well explained by LAI (~90%). It should be noted that P_{LAI} here not only included leaf-level photosynthesis but also included how different models treat the canopy. The big leaf model and the sunlit/shaded leaf model could have similar leaf-level photosynthesis but different P_{LAI}. The variations in leaf-level photosynthesis and variations in scaling-up from leaf to canopy jointly controlled the fluctuations of P_{LAI}. For sunlit/shaded leaf models (only 4 of 12 models that provided LAI outputs; Table S2), P_{LAI} was defined as the average LAI-level photosynthesis of sunlit and shaded leaves.

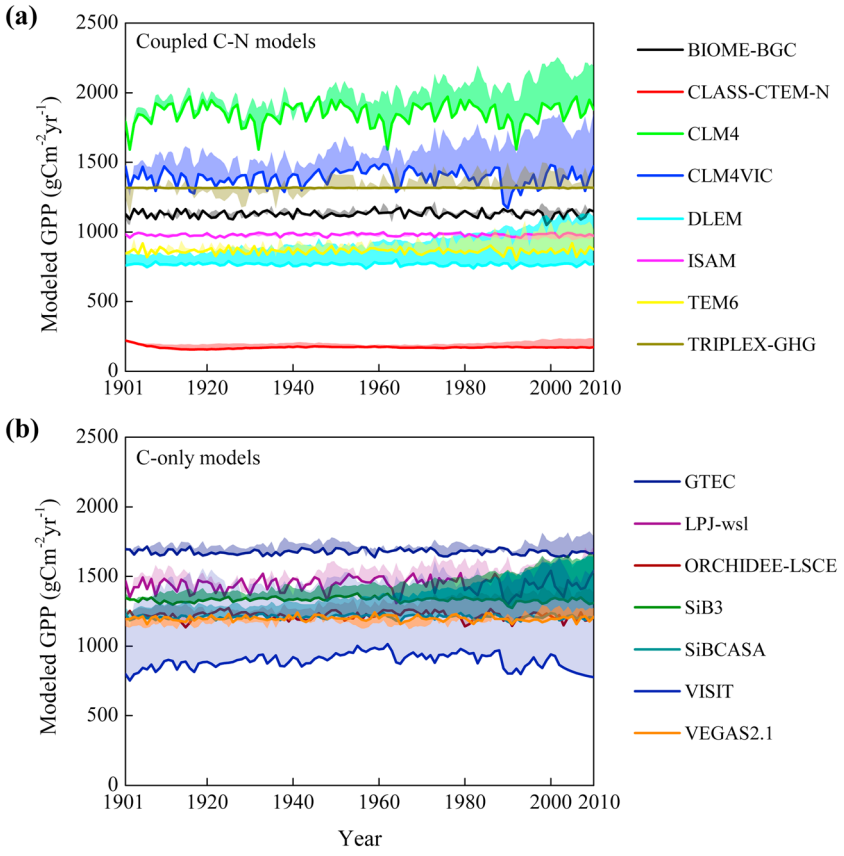

Figure 3. Yearly averaged GPP from initial condition (with constant environment conditions: solid line) and under environmental changes (shade outline) for coupled C-N models (a) and C-only models (b). The shades show the effects of environmental drivers (positive above the solid lines, and negative below the solid lines).

For a better understanding of plant functional properties in controlling the intermodel difference of simulated GPP, we applied a relative importance algorithm (see section 2) to attribute the inter-model variation in GPP. In each grid cell, we fit the data to a multiple linear regression ($GPb_0+b_1 \times CUE+b_2 \times \tau_{veg}+b_3 \times F_{leaf}+b_4 \times SLA+b_5 \times P_{LAI}$). Then the relative importance of each variable was estimated by splitting the total correlation coefficient (R^2; Figure S7) of multiple linear regression. Finally, the relative importance of each variable was normalized (divided by R^2) to sum to 1. The factors that made the greatest contribution to GPP variation was identified as the dominant driver. Spatially, intermodel variation of GPP in around 85% of the areas could be explained by the difference in SLA (54%), F_{leaf} (17%), and P_{LAI} (14%). The attribution analysis further proved that large spread in modeled GPP predominantly resulted from differences of SLA and F_{leaf} among models.

3.3. Model sensitivity to the Changing Environmental Drivers

All of the models showed that the modeled annual GPP was relatively stable during 1901–1960, while a significant increase occurred after the sixtieth over the East Asian Monsoon region. Based on the outputs from different simulation experiments, we found that the increase of ensemble mean GPP predominantly resulted from increasing atmospheric CO_2 concentration and nitrogen deposition, while the effect of climate forcing was nearly neutral (Figure 5a). Land-use change during the past century showed a slightly negative effect on GPP and partly counteracted the effects of other environmental drivers. There are large model-to-model differences in both the direction and magnitude of the effects induced by climate forcing and land-use change. Furthermore, the trends in GPP driven by climate forcing, atmospheric CO_2, land-use change and nitrogen deposition were computed by using segmented linear regression breaking at the sixtieth (Zhu et al., 2017). The model factorial simulations suggested that the dominant environmental drivers were consistent

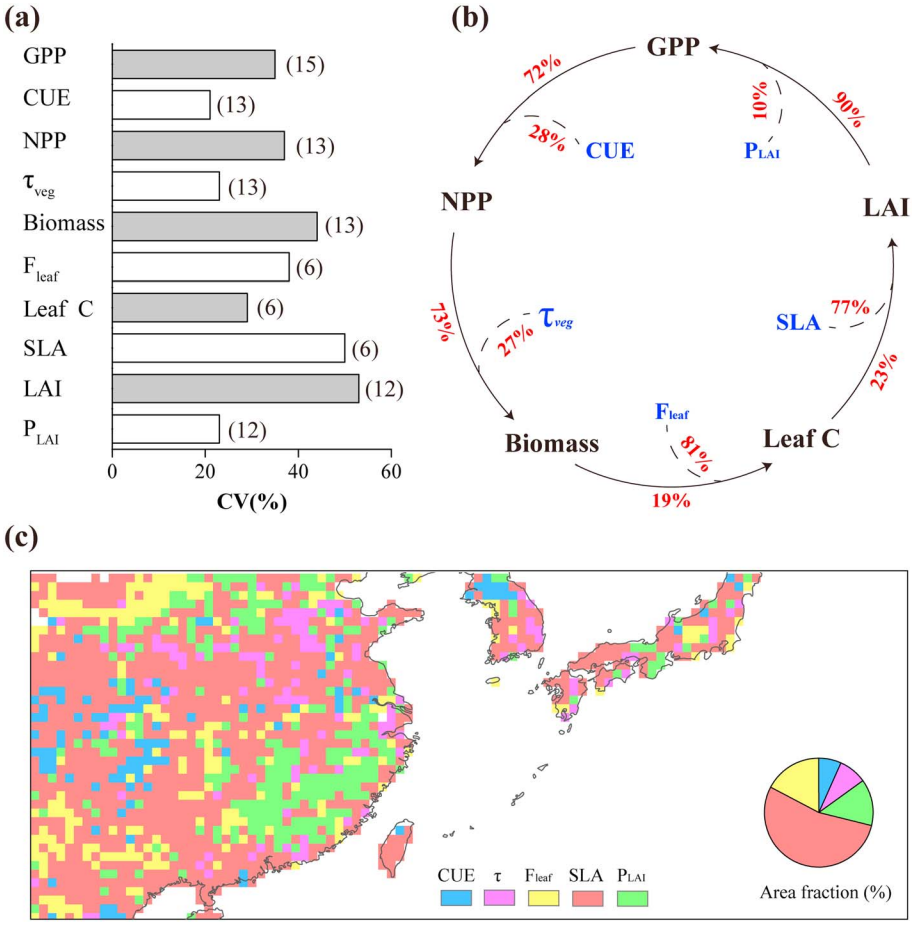

Figure 4. (a) Intermodel variability (coefficient of variation: CV = 100% × SD/mean) of key carbon processes and vegetation functional properties. Numbers behind the bars indicate the number of models provide outputs for the carbon processes and vegetation functional properties. (b) Relative importance of key carbon processes and the associated vegetation functional properties in controlling model performance on GPP. (c) Contributions of the five vegetation functional properties in driving GPP.

during 1901–2010 (Figure 5b). The dramatic environmental changes after the sixtieth significantly shaped the dynamic in GPP, CO_2 fertilization was the largest contributor to the modeled GPP trend (1.89 ± 0.47 g $C{\cdot}m^{-2}{\cdot}year^{-1}$ for coupled C-N models and 3.36 ± 0.92 g C m^{-2} $year^{-1}$ for C-only models), followed by nitrogen deposition (1.62 ± 1.71 g $C{\cdot}m^{-2}{\cdot}year^{-1}$), land-use change (−0.92 ± 0.93 g $C{\cdot}m^{-2}{\cdot}year^{-1}$ for coupled C-N models and −0.28 ± 1.88 g $C{\cdot}m^{-2}{\cdot}year^{-1}$ for C-only models), and climate forcing (0.14 ± 0.74 g $C{\cdot}m^{-2}{\cdot}year^{-1}$ for coupled C-N models and 0.80 ± 0.66 g $C{\cdot}m^{-2}$ $year^{-1}$ for C-only models; Figure 5b). On average, the C-N cycle models lead to a dampened sensitivity of GPP to atmospheric CO_2 and historical climate change, and this weaker response was consistent with the global results (Huntzinger et al., 2017). This large difference of atmospheric CO_2 effect between coupled C-N models and C-only models might due to the unrealistic unconstrained CO_2 fertilization response in C-only models. But it is hard to say whether this unrealistic constraint resulted from N availability or other structural differences. However, the effects of nitrogen deposition should be interpreted with caution, because only seven of the models performed the factorial simulations with and without nitrogen cycling (Table S2).

The models differently simulated the contributions of environmental factors in driving the increasing trend of GPP across the East Asian monsoon region. This was largely due to their different representations of the environmental impacts on vegetation functional properties among models. The model factorial simulations suggested that the effect of climate forcing on vegetation functional properties was much lower than other

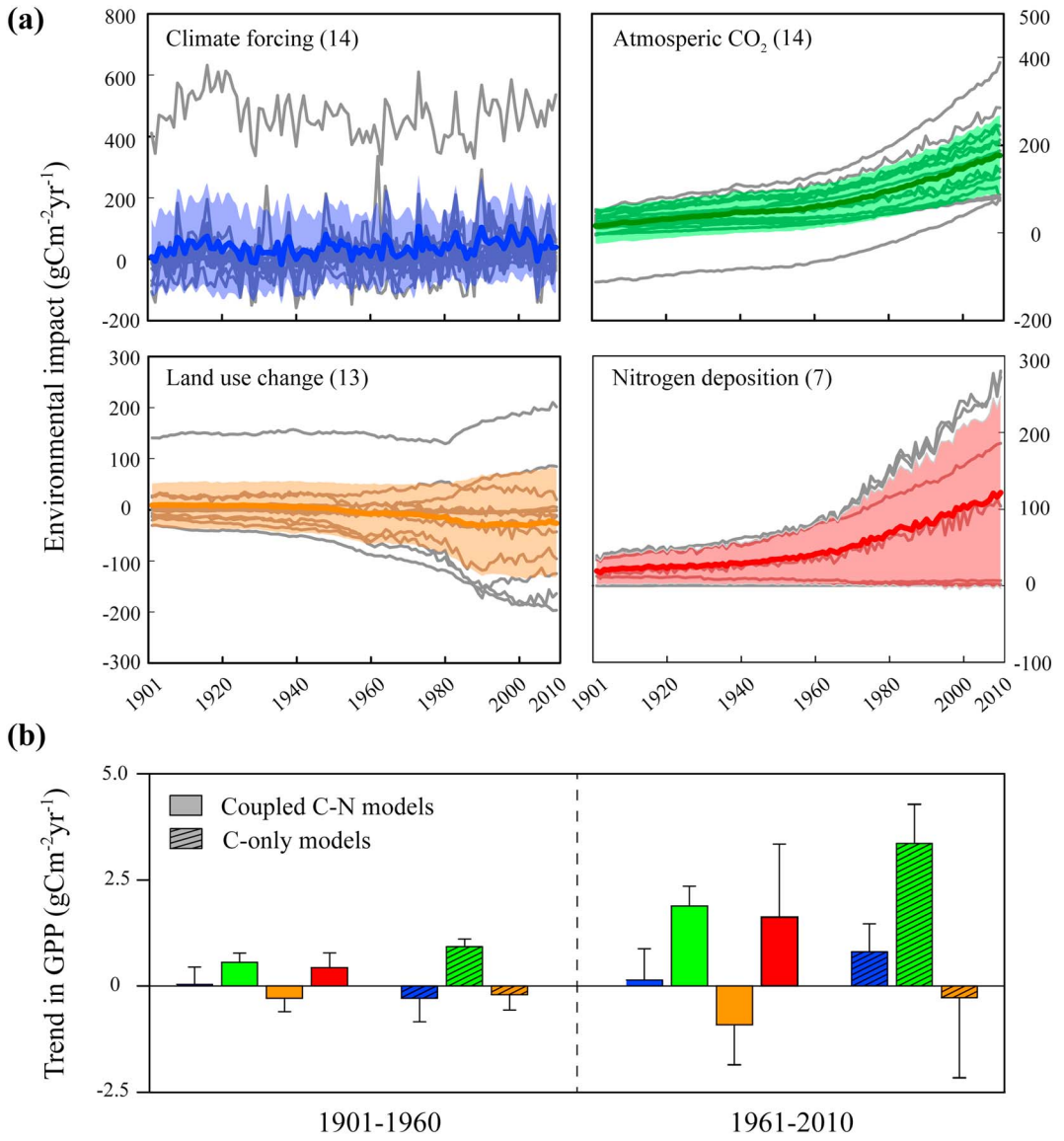

Figure 5. (a) The impact of climate forcing, atmospheric CO_2, land-use change and nitrogen deposition on the dynamics of GPP in the East Asian monsoon region between 1901 and 2010. The gray lines are results from individual models, and the bold colored lines and the shaded areas are respectively the calculated average and standard deviation among models. The number of models is shown in parentheses. (b) Trends in GPP driven by climate forcing, atmospheric CO_2, land-use change and nitrogen deposition using segmented linear regression breaking at the sixtieth. Error bars show the standard deviation among models.

environmental factors (Figure 6a). Increasing CO_2 had a positive effect on most vegetation functional properties, but lead to a significant decrease of F_{leaf} (Figure 6b). Land-use change also stimulated the increase of most vegetation functional properties, but negatively affected GPP mainly by reducing τ_{veg} (Figure 6c). The positive contribution of nitrogen deposition to GPP was mainly attributed to the increase of F_{leaf} and SLA (Figure 6d). In addition, τ_{veg}, F_{leaf}, and SLA were more sensitive to environmental changes with the relative higher response ratios. The response of τ_{veg} to climate forcing and atmospheric CO_2 remained highly uncertain, while intermodel variation of the land-use change and nitrogen deposition effect was greatest in CUE. Overall, model representation and integration of these properties' individual and combined responses to environmental drivers will be critical to capture whole system responses.

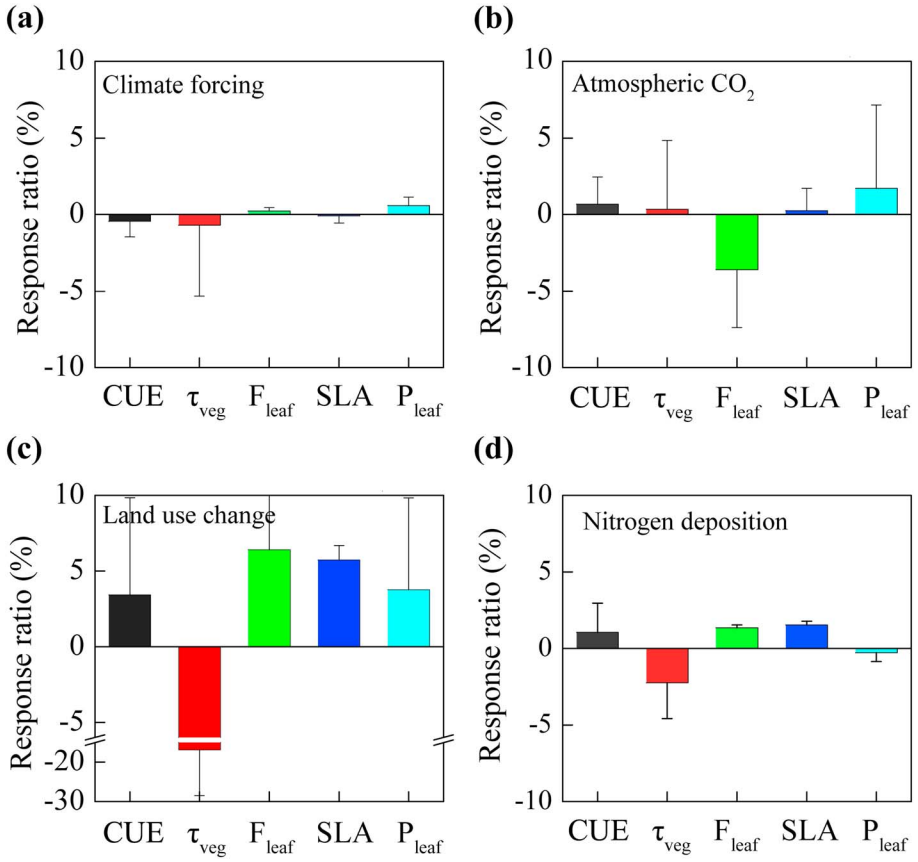

Figure 6. The simulated response ratios of vegetation functional properties to climate forcing (a), atmospheric CO_2 (b), land-use change (c) and nitrogen deposition (d). Error bars show the standard deviation of response ratios among models.

3.4. Comparison of Modeled Variables Against Observation-Based Products

The performances of 15 TBMs in simulating the GPP, NPP, LAI, and aboveground biomass C were evaluated against the satellite-derived and data-oriented products. Analysis was carried out on years overlapping with the observation periods at 0.5° × 0.5° resolution. As shown in Figure 7, the position of each letter appearing in the plot represents how closely that model's simulation matches the satellite-derived/data-oriented value. Presented by Taylor diagram, the SD ratios of TBMs ranging from 0.42 to 1.98, and 9 out of 15 models overestimate the GPP spatial amplitude over the East Asian Monsoon region. The models showed correlation coefficient (R) between 0.32 and 0.94, indicating substantial variations in how well they captured the spatial pattern in annual GPP. Four models (i.e., DLEM, ORCHIDEE-LSCE, ISAM, and LPJ-wsl) had SD ratios near 1.0, which suggests these models have similar magnitudes of spatial variation with the MODIS GPP and MTE GPP (Figure 7a). The modeled NPP showed large disagreement on the spatial pattern with the MODIS NPP but fit the MTE NPP well, with the corresponding R ranging from 0.15 to 0.6 and 0.2 to 0.9, respectively. In addition, the models produced comparable SDs of NPP among all grid cells to the MODIS NPP and MTE NPP, with most of the models had SD ratios near 1.0 (Figure 7b). None of the models in this study achieved a good overall performance of root-mean-square error less than one for the aboveground biomass C (Figure 7c). Most of the models overestimated the magnitude of spatial variation in LAI, with the SD ratios larger than 1.0 (Figure 7d). Ten out of eleven models had $R > 0.5$ for LAI, indicating that the modeled spatial patterns of LAI were comparable to the satellite-derived products.

A large number of field observations and data-oriented products provide continuous and effective benchmarks to assess modeled vegetation functional properties (CUE, τ_{veg}, F_{leaf}, and SLA; Figure 8a). Spatially, the modeled vegetation functional properties had very low correspondence with observations

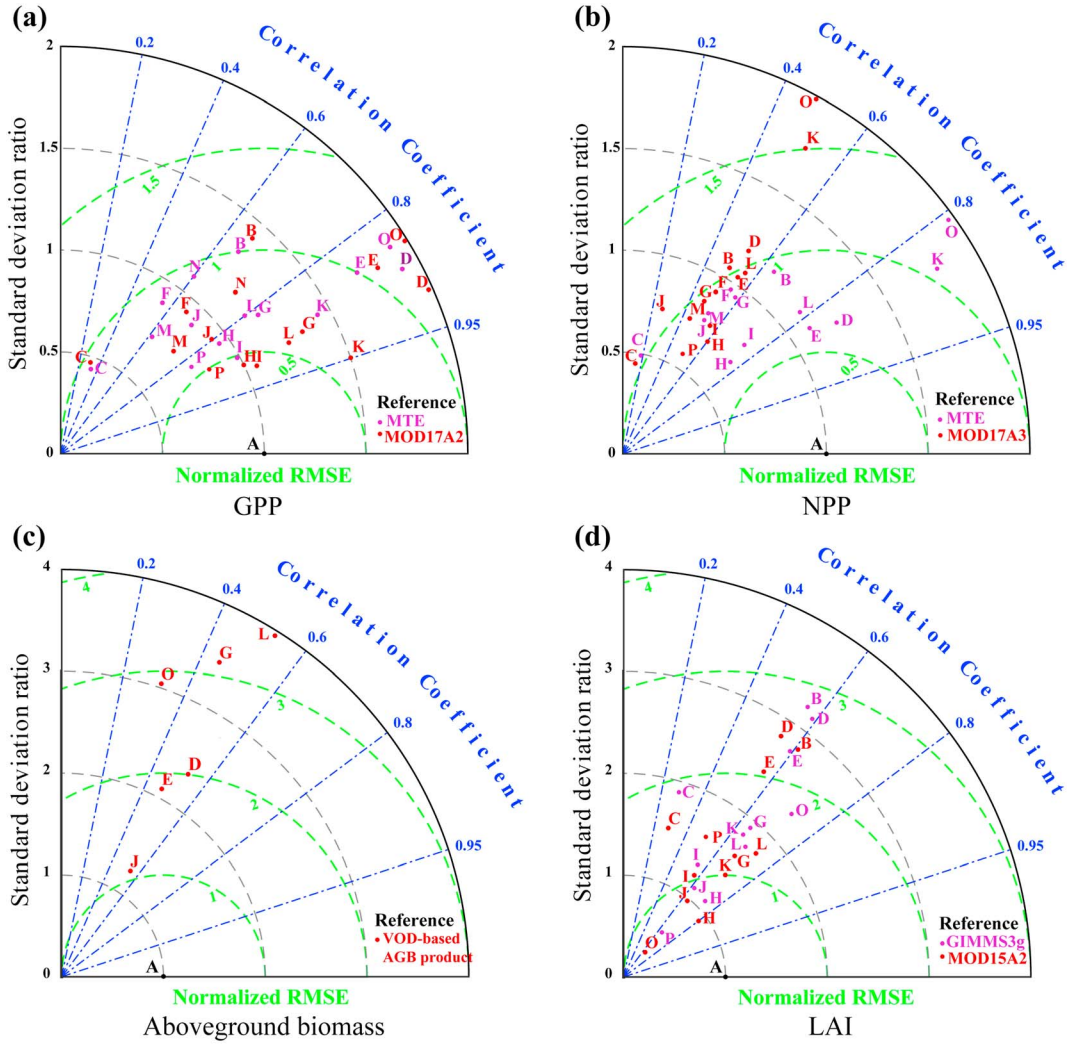

Figure 7. Taylor plots by Multi-scale Synthesis and Terrestrial Model Intercomparison Project models for (a) GPP, (b) NPP, (c) aboveground biomass carbon, and (d) LAI. The correlation coefficient measures how well the simulated fluxes capture the spatial distribution of the observed fluxes. The radial direction is the ratio of simulated to observed standard deviation. The green lines represent root-mean-square error (RMSE) normalized by standard deviation. An ideal model would have a standard deviation ratio of 1.0 and a correlation of 1.0 (point A).

(Figures 8b–8e). Large disagreement of F_{leaf} may result from the mechanized allocation strategy, that is, some of the models preset a max LAI threshold beyond which no allocation of biomass to leaves (Table S2). In reality, the leaf fraction will be changing as a function of age, having a large value for young forest and a small value for mature forest (Reich et al., 2014). In addition, τ_{veg} is also closely related to forest age and soil nutrient (Wang, Sun, et al., 2017). However, the effects of forest age are rarely considered in current models. The spatial mismatch between the modeled SLA and environmental drivers-based SLA may be due to the PFT-based parameterization process in models, which was poorly situated to capture key differences within PFT and the effects of environmental filtering (Yang et al., 2015). Our study presented a range of modeled CUE between 0.35 and 0.65, while the observed CUE showed higher variability (Figures 8e and S8). Such underestimated variation of CUE in the models also been detected in

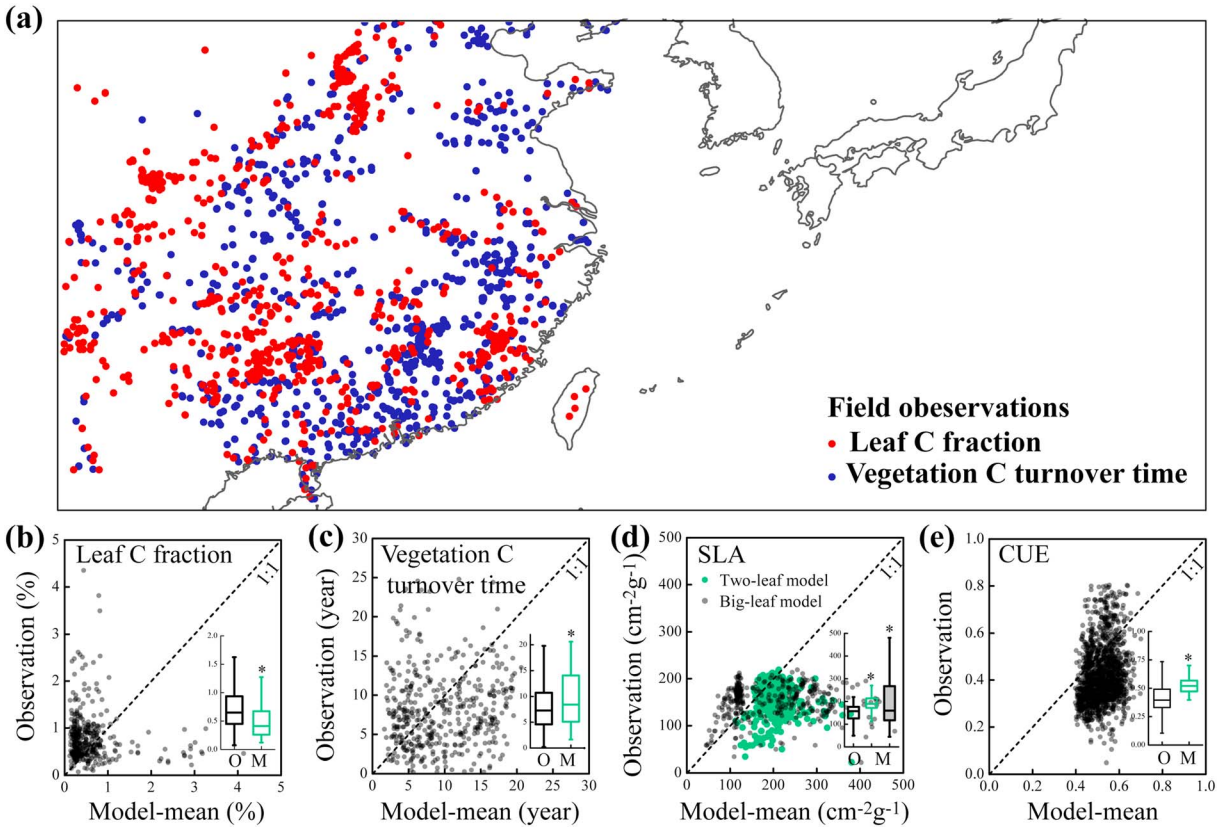

Figure 8. (a) The location of observations in the assemble database of leaf C fraction and vegetation C turnover time. (b–e) Comparison of model-derived and observation-based leaf C fraction, vegetation C turnover time, specific leaf area and C-use efficiency. The asterisk (*) represents the statistical significance at $p < 0.05$.

the permafrost regions by Xia et al. (2017). The low variability of modeled CUE is likely associated with a simplistic representation of plant respiration in models. However, improving the simulation of respiration in current models is still challenging (Atkin et al., 2015). As shown in Table S7, the maintenance respiration (R_m) is closely related with different plant functional properties in models (e.g., LAI in ORCHIDEE, tissue-specific nitrogen content in CLM4.5, and V_{max} in CLASS; Arora, 2003; Krinner et al., 2005; Oleson et al., 2013). In addition, the growth respiration (R_g) is defined as divergent ratio of the total carbon in new growth (20–30%; Clein et al., 2007; Ito et al., 2007; Sitch et al., 2003). Furthermore, the temperature limitation on carbon sink for assimilates in the plant is probably missing in models (Fatichi et al., 2014). Thus, more research is still needed on the exploration of the underlying mechanisms regulating variability of plant respiration and therefore CUE. The comparison analysis suggested more research is still needed to improve the spatial representation of plant functional properties in current models.

In addition, the modeled τ_{veg}, SLA and CUE were significantly higher than those calculated from observation-based datasets, suggesting overestimates of CUE (18.1±21.3%), τ_{veg} (18.2±26.9%), and SLA (29.8±9.9% in two-leaf models and 25.9±16.9% in big-leaf models) by MsTMIP models in the East Asian Monsoon region. Conversely, F_{leaf} was significantly underestimated by models (21.7±52.2%).

4. Discussion

4.1. Improving GPP Simulation With Initial Vegetation States

Previous studies have identified relevant sources of uncertainty for predicting terrestrial ecosystem productivity, such as vegetation properties (Walker et al., 2017), initial conditions (Carvalhais et al., 2010; Carvalhais et al., 2010), and environmental response (Rollinson et al., 2017; Wu et al., 2017). Here we show that the intermodel variation of terrestrial ecosystem productivity in the East Asian Monsoon region critically depends on their initial representations of GPP-related processes and vegetation functional

properties rather than their different simulations of environmental impacts. The difference of simulated GPP at the initial condition will propagate to not only the historical simulations but also the future predictions with different climate scenarios. This could be one important reason for the commonly reported large intermodel variation of GPP for both historical and scenario-based simulations in almost all existing MIPs, such as TRENDY (Peng et al., 2015), Coupled Model Intercomparison Project Phase 5 (Anav et al., 2013), C4MIP (Qian et al., 2010), and ISI-MIP2a (Ito et al., 2017). In fact, this propagation of model uncertainty begins from initial conditions also existed in the simulation of soil organic C by current Earth system models (Exbrayat et al., 2014; Todd-Brown et al., 2014). These findings together suggest a high priority to reduce model difference in the initial conditions of terrestrial C cycle in current TBMs.

Intermodel disagreement of ecosystem production based on divergence in initial condition is difficult to diagnose and reduce, mainly because of the fast propagation of simulation uncertainty among the internal processes. We have identified that the large spread of modeled GPP predominantly resulted from differences in LAI and SLA among models. The underlying error in simulated GPP will then propagate through the GPP-simulation loop and introduce some additional errors in subsequent transmission processes carbon assimilation (e.g., NPP, carbon allocation, and leaf area dynamics; Rogers et al., 2017). Therefore, the initial parameterization of leaf-level functional properties is critical to ensure the reliable values of terrestrial carbon cycle.

4.2. Model Uncertainty on Vegetation Functional Properties and Their Responses to Environmental Changes

The large spread of initial conditions predominantly resulted from the difference in vegetation functional properties (e.g., CUE, τ_{veg}, F_{leaf}, and SLA) among models. The modeled ensemble mean functional properties were larger than the observations, and these properties vary largely among different models. Most of the current TBMs condense functional diversity to PFTs with parameterized properties (Sakschewski et al., 2015), thus allowing for only limited variation and similar responses patterns to environmental changes within and between PFTs (Kunstler et al., 2016; Reichstein et al., 2014). In fact, there is substantial inter and intraspecific functional variation that will largely affect community assembly and vegetation-atmosphere carbon exchange. PFTs were poorly situated to capture key differences in plant traits across species (Anderegg, 2014). Some recent studies have suggested that greater effort is needed to understand variation of field plant traits and assess the uncertainties of different upscaling methods (Musavi et al., 2015; Walker et al., 2017). In the GPP-simulation loop, we used F_{leaf} instead of NPP allocation representing plants partitioning strategy. Here F_{leaf} can be regarded as a model-derived functional property that reflects the integrated effect of new biomass allocation and max LAI threshold in models. Accumulation of plant biomass is a function of NPP, allocation, and mortality (turnover time), but most forests, once they reach a closed canopy state, continue to accumulate woody biomass without undergoing commensurate increases in leaf C. Therefore, the leaf fraction will be changing as a function of age. The field observations indeed proved a larger F_{leaf} value for young forest and a smaller F_{leaf} value for mature forest (Figure 9a). However, the general pattern of the age-related changes F_{leaf} could be captured by CLM4 and CLM4VIC, which have no maximal LAI limitation, but not shown in some models (e.g., ORCHIDEE and VISIT) with the max-LAI threshold (Figures 9b–9g). Thus, we suggested that the age-dependence of biomass and NPP allocation need improvements in the forest carbon cycle modeling.

Moreover, the terrestrial ecosystem in the East Asian Monsoon region is strongly shaped by anthropogenic perturbations in terms of species composition and community structure in recent years (Qin et al., 2016; Yang et al., 2015). However, most of the models do not simulate human management including fertilization and irrigation (Tian et al., 2003). Some models still use potential vegetation map or treat cropland as grassland, which to a large extent explains the large divergence in initial vegetation properties. Furthermore, we still have limited understanding of the natural plasticity of these properties under considerable environmental changes in the future (Verheijen et al., 2013). Overall, a more realistic representation of vegetation functional properties, with the consideration of their biogeographical and ecological variability, would improve the simulation and prediction of GPP in the East Asian monsoon region. Reducing the simulation biases on environmental impacts on vegetation functional properties is urgently needed in the East Asian monsoon region. The importance of improved CUE in current TBMs has been highlighted by a recent model evaluation on ecosystem productivity over the northern permafrost regions (Xia et al., 2017). This study also

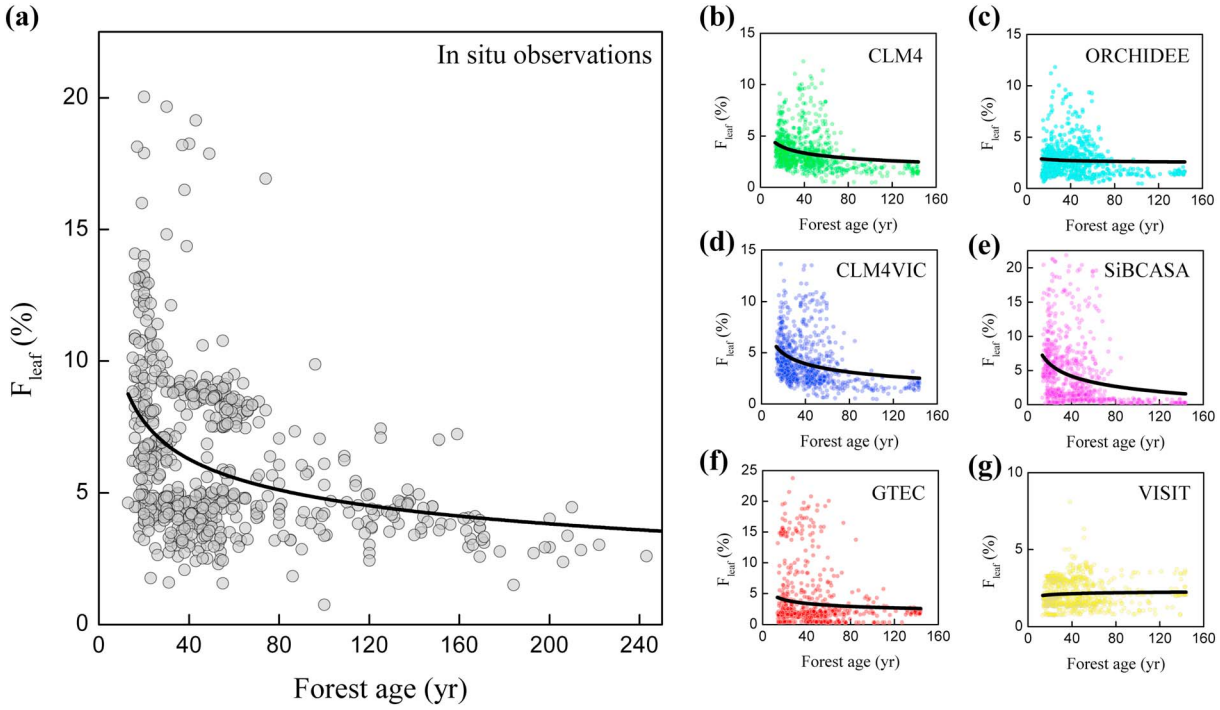

Figure 9. Age-related dynamics of leaf C fraction from field observations (a) and Multi-scale Synthesis and Terrestrial Model Intercomparison Project models (b–g).

supports the analysis of ISI-MIP models (Friend et al., 2014), which found that τ_{veg} is one major uncertainty source for simulating long-term dynamics of terrestrial ecosystem productivity. The CO_2-induced decrease of F_{leaf} could be attributed to the increased plant demand for nutrients with a larger carbon allocation to roots (Poorter et al., 2012). However, our confidence in the modeled impacts of increasing CO_2 concentration and nitrogen deposition is low. This is because experimental evidence on CO_2 effects in the East Asian monsoon region is scarce (Figure S2), and there are inconsistent findings for N effects on P_{LAI} (Mao et al., 2015; Strengbom & Reich, 2006). Fortunately, a large number of global change manipulative experiments have been conducted in this region to test the vegetation response to environmental changes (Fu et al., 2015). Nitrogen addition was the most frequently manipulated treatment, identified in 28 of the total 49 experiments, while other treatments were only manipulated in limited experiments (Table S8 and Figure S10). The utility of these experiments for constraining responses in models may be controversial, as the mismatch of the corresponding vegetation properties and environmental drivers, the limited duration to induce critical feedbacks (Luo et al., 2011). Globally, the FACE-MDS project, incorporating synchronous simulated and experimental results, provide valuable guidance in identifying critical model assumptions (Medlyn et al., 2015). However, the universality of these assumptions needs more validation for the limited climate space and biodiversity (Norby et al., 2016). We encourage the application of such MDS or "assumption-centered" approach in the East Asian monsoon region to fundamentally improve understanding of feedbacks between terrestrial ecosystem and the atmosphere accompanied by subtropical monsoon.

4.3. Overestimated GPP and Implications for Data-Model Integration in the East Asian Monsoon Region

Many previous studies have reported the overestimation of global or regional GPP by current TBMs (Peng et al., 2015; Xia et al., 2017; Yao et al., 2017). In the East Asian monsoon region, such model overestimation is mainly attributable to the overestimation of vegetation functional properties (especially in SLA and LAI). The modeled CUE in the East Asian monsoon region (52±1%) is higher than those derived from global gridded data products (44±2%) and globally distributed in situ measurements across 131 sites (46±1%; Campioli et al., 2015). However, the observation-based CUE was calculated from two dependent data

products, which may generate some uncertainty for estimating the CUE. To avoid the effect of autocorrelation, we also calculated the CUE values from MTE GPP (Jung et al., 2011) and MODIS NPP and this overestimation trend was still validated (Figure S8). The overestimation of τ_{veg} in the East Asian Monsoon region was also found in global vegetation models participating in ISI-MIP (Thurner et al., 2017). Long-term satellite-derived LAI products (MOD15A2-LAI, GLOPMAP-LAI, GLASS-LAI, GIMMS3g LAI, etc.) are often used to evaluate the models. However, a relatively large discrepancy among these long-term LAI products has also been reported in some recent studies (Xiao et al., 2017; Zhu et al., 2017). Therefore, the uncertainty of LAI data itself (Jiang et al., 2017) should be considered when evaluating model performances.

The positive GPP bias does not necessary mean the ecosystem C sink is also overestimated by current TBMs in the East Asian monsoon region. Conversely, a recent study showed that current models tend to underestimate NEP fivefold to sevenfold (Yu et al., 2014), consistent with the results computed from MsTMIP models (Figure S9). The diametrically opposed performance of models in simulating GPP and NEP reveals that the modeled ecosystem respiration has a larger relative bias compared to GPP. This large "missing" or "residual" terrestrial carbon sink may be due to the lateral flows of sequestered C to aquatic ecosystems, which is rarely considered in most of the current TBMs. Recent evidence has suggested that this non-biological process sustains an important C sinks in this region (Li et al., 2017). Therefore, we recommend the inclusion of dissolved C coupled with hydrologic processes in the modeled soil C cycling. In addition, a more accurate prediction of the C sink dynamic in the East Asian monsoon region requires more observations of specific processes linked to both ecosystem C uptake and losses in this region.

The multiple observational networks in the East Asian monsoon region can potentially provide useful benchmarks for the TBMs (Figure S10). For example, there are currently 78 flux towers in the East Asian monsoon region (Tables S9 and S10), which could offer reliable benchmarks for the modeled dynamics of C and water processes in terrestrial ecosystems (He et al., 2010; Ichii et al., 2013). The Center for Tropical Forest Science and Forest Global Earth Observatories (CTFS-ForestGEO) is a global network of forest research plots, and has established 12 large permanent forest plots in the East Asian monsoon region to monitor the long-term changes of vegetation and species coexistence (Table S11; Cao et al., 2013; Chao et al., 2010; Chen, 2009; Ding et al., 2013; Feng et al., 2016; Guo et al., 2015; Hau et al., 2005; Lan et al., 2009; Lu et al., 2013; Song et al., 2015; Su et al., 2007; Yang et al., 2011; Chang et al., 2012). These observational networks, together with the field experiments, could be excellent platforms to improve the modeling of vegetation functional properties in the East Asian monsoon region.

5. Conclusions

In conclusion, we identified the uncertainty sources of intermodel differences and model ensemble biases in the simulated GPP across the East Asian monsoon region. The limitations of different presentations of plant traits among current models have been widely discussed by recent studies (Anderegg et al., 2014; Verheijen et al., 2013). This study identified the dominant roles of SLA (LAI) and F_{leaf} in the simulated intermodel variation of GPP. In addition, the model ensemble overestimation in simulated GPP in the East Asian monsoon region was mainly attributed to the relatively higher modeled SLA and CUE. The field measurements showed that F_{leaf} changes as a function of age but the observed age-related pattern was not well captured by these models. Thus, we suggest a high priority to add the age dependence of biomass and NPP allocations into the current models. Our traceability framework is applicable to most existing MIPs to diagnose the sources of intermodel variability in simulated GPP. Furthermore, some key questions need to be addressed in future researches. First, only C-related vegetation functional properties were included in this framework. It remains unclear how simulated GPP simulation is impacted by those water- and nutrient-related properties among models (Reichstein et al., 2014). Second, large differences in the vegetation functional properties among models should be attributed to the diverse representations of PFT maps and the inconsistent parameterizations of functional properties within the same PFT (Bloom et al., 2016; Xia et al., 2017). The relative contributions of PFT maps and inconsistent parameters to the intermodel difference in vegetation functional properties need to be further quantified. Overall, this study highlights that the modeling of ecosystem productivity at middle-to-low latitudes could benefit from a better understanding of the biogeographical and ecological variations in plant traits and vegetation functional properties.

Acknowledgments
This work was financially supported by the National Key R&D Program of China (2017YFA0604603), National Natural Science Foundation of China (31722009, 41630528), the Fok Ying-Tong Education Foundation for Young Teachers in the Higher Education Institutions of China (Grant 161016), and National 1000 Young Talents Program of China. Funding for the Multiscale synthesis and Terrestrial Model Intercomparison Project (MsTMIP; https://nacp.ornl.gov/MsTMIP.shtml) activity was provided through NASA ROSES Grant NNX10AG01A. Data management support for preparing, documenting, and distributing model driver and output data was performed by the Modeling and Synthesis Thematic Data Center at Oak Ridge National Laboratory (ORNL; http://nacp.ornl.gov), with funding through NASA ROSES Grant NNH10AN681. Finalized MsTMIP data products are archived at the ORNL DAAC (http://daac.ornl.gov). We also acknowledge the modeling groups that provided results to MsTMIP and their funding sources. J. B. F. contributed to this work from the Jet Propulsion Laboratory, California Institute of Technology, under a contract with the National Aeronautics and Space Administration. California Institute of Technology, Government sponsorship acknowledged. TRIPLEX-GHG: TRIPLEX-GHG was developed at University of Quebec at Montreal (Canada) and Northwest A&F University (China) and has been supported by the National Basic Research Program of China (2013CB956602) and the National Science and Engineering Research Council of Canada (NSERC) Discover Grant. C. L. M: This research is supported in part by the US Department of Energy (DOE), Office of Science, Biological and Environmental Research. Oak Ridge National Laboratory is managed by UT-Battelle, LLC for DOE under contract DE-AC05-00OR22725. The authors declare that the data supporting the finding of this study are available within the article and its supporting information files. Model results are available from the MsTMIP Global Simulation Results version 1.0. The URL for the data is https://doi.org/10.3334/ORNLDAAC/1225. The MODIS GPP/NPP data were provided by the Numerical Terradynamic Simulation Group (NTSG) at the University of Montana (ftp://ftp.ntsg.umt.edu/pub/MODIS/NTSG_Products/https://lpdaac.usgs.gov/dataset_discove-ry/modis/modis_products_table/mod17a3). MTE GPP estimates used in this study are available from Jung et al., 2011; https://doi.

References

Allen, R. G., Pereira, L. S., Raes, D., & Smith, M. (1998). Crop evapotranspiration—Guidelines for computing crop water requirements, FAO irrigation and drainage paper 56, Food and Agriculture Organization of the United Nations, Rome. http://www.fao.org/docrep

Anav, A., Friedlingstein, P., Beer, C., Ciais, P., Harper, A., Jones, C., et al. (2015). Spatiotemporal patterns of terrestrial gross primary production: A review. *Reviews of Geophysics*, *53*, 785–818. https://doi.org/10.1002/2015RG000483

Anav, A., Friedlingstein, P., Kidston, M., Bopp, L., Ciais, P., Cox, P., et al. (2013). Evaluating the land and ocean components of the global carbon cycle in the CMIP5 Earth system models. *Journal of Climate*, *26*(18), 6801–6843. https://doi.org/10.1175/JCLI-D-12-00417.1

Anderegg, W. R. (2014). Spatial and temporal variation in plant hydraulic traits and their relevance for climate change impacts on vegetation. *New Phytologist*, *205*(3), 1008–1014. https://doi.org/10.1111/nph.12907

Arora, V. K. (2003). Simulating energy and carbon fluxes over winter wheat using coupled land surface and terrestrial ecosystem models. *Agricultural and Forest Meteorology*, *118*(1-2), 21–47. https://doi.org/10.1016/S0168-1923(03)00073-X

Atkin, O. K., Bloomfield, K. J., Reich, P. B., Tjoelker, M. G., Asner, G. P., Bonal, D., et al. (2015). Global variability in leaf respiration in relation to climate, plant functional types and leaf traits. *New Phytologist*, *206*(2), 614–636. https://doi.org/10.1111/nph.13253

Baker, I. T., Prihodko, L., Denning, A. S., Goulden, M., Miller, S., & Rocha, H. R. D. (2008). Seasonal drought stress in the Amazon: Reconciling models and observations. *Journal of Geophysical Research*, *113*, G00B01. https://doi.org/10.1029/2007JG000644

Beer, C., Reichstein, M., Tomelleri, E., Ciais, P., Jung, M., Carvalhais, N., et al. (2010). Terrestrial gross carbon dioxide uptake: global distribution and covariation with climate. *Science*, *329*(5993), 834–838. https://doi.org/10.1126/science.1184984

Bloom, A. A., Exbrayat, J. F., Ir, V. D. V., Feng, L., & Williams, M. (2016). The decadal state of the terrestrial carbon cycle: Global retrievals of terrestrial carbon allocation, pools, and residence times. *Proceedings of the National Academy of Sciences of the United States of America*, *113*(5), 1285–1290. https://doi.org/10.1073/pnas.1515160113

Bunker, D. E., Declerck, F., Bradford, J. C., Colwell, R. K., Perfecto, I., Phillips, O. L., et al. (2005). Species loss and aboveground carbon storage in a tropical forest. *Science*, *310*(5750), 1029–1031. https://doi.org/10.1126/science.1117682

Campioli, M., Vicca, S., Luyssaert, S., Bilcke, J., Ceschia, E., Chapin, F. S. III, et al. (2015). Biomass production efficiency controlled by management in temperate and boreal ecosystems. *Nature Geoscience*, *8*(11), 843–846. https://doi.org/10.1038/ngeo2553

Cao, H., Wu, L., Wang, Z., Huang, Z., Li, L., Wei, S., et al. (2013). *Dinghushan lower subtropical forest dynamics plot: Tree species and their distribution patterns (in Chinese with English abstract)*. Beijing: China Forestry Publishing House.

Carvalhais, N., Reichstein, M., Ciais, P., Collatz, G. J., Mahecha, M. D., Montagnani, L., et al. (2010). Identification of vegetation and soil carbon pools out of equilibrium in a process model via eddy covariance and biometric constraints. *Global Change Biology*, *16*(10), 2813–2829. https://doi.org/10.1111/j.1365-2486.2010.02173.x

Carvalhais, N., Reichstein, M., Collatz, G. J., Mahecha, M. D., Migliavacca, M., Neigh, C. S. R., et al. (2010). Deciphering the components of regional net ecosystem fluxes following a bottom-up approach for the Iberian Peninsula. *Biogeosciences*, *7*(11), 3707–3729. https://doi.org/10.5194/bg-7-3707-2010

Chang, L. W., Chiu, S. T., Yang, K. C., Wang, H. H., Hwong, J. L., & Hsieh, C. F. (2012). Changes of plant communities classification and species composition along the micro-topography at the Lienhuachih Forest Dynamics Plot in the central Taiwan. *Taiwania*, *57*(4), 359–371. https://doi.org/10.6165/tai.2012.57.359

Chao, W.-C., Song, G.-Z. C., Chao, K.-J., Liao, C.-C., Fan, S.-W., Wu, S.-H., et al. (2010). Lowland rainforests in southern Taiwan and Lanyu, at the northern border of Paleotropics and under the influence of monsoon wind. *Plant Ecology*, *210*(1), 1–17. https://doi.org/10.2307/40802412

Chen, B. (2009). *Gutianshan forest dynamics plot: Tree species and their distribution patterns (in Chinese with English abstract)*. Beijing: China Forestry Publishing House.

Chen, Z., Yu, G., Ge, J., Sun, X., Hirano, T., Saigusa, N., et al. (2013). Temperature and precipitation control of the spatial variation of terrestrial ecosystem carbon exchange in the Asian region. *Agricultural and Forest Meteorology*, *182-183*, 266–276. https://doi.org/10.1016/j.agrformet.2013.04.026

Clein, J., Mcguire, A. D., Euskirchen, E. S., & Calef, M. (2007). The effects of different climate input datasets on simulated carbon dynamics in the western Arctic. *Earth Interactions*, *11*(12), 1–24. https://doi.org/10.1175/EI229.1

Cox, P. M., Pearson, D., Booth, B. B., Friedlingstein, P., Huntingford, C., Jones, C. D., & Luke, C. M. (2013). Sensitivity of tropical carbon to climate change constrained by carbon dioxide variability. *Nature*, *494*, 341–344. https://doi.org/10.1038/nature11882

Ding, B., Chen, D., Luo, Z., Chen, X., Hu, R., Ye, Z., Wang, W., et al. (2013). *Zhejiang Baishanzu forest dynamics plot: Tree species and their distribution patterns (in Chinese with English abstract)*. Beijing: China Forestry Publishing House.

Du, Q., Liu, H. Z., Feng, J. W., Wang, L., Huang, J. P., Zhang, W., & Bernhofer, C. (2012). Carbon dioxide exchange processes over the grassland ecosystems in semiarid areas of China. *Science China Earth Sciences*, *55*(4), 644–655. https://doi.org/10.1007/s11430-011-4283-1

Du, Z., Weng, E., Jiang, L., Luo, Y., Xia, J., & Zhou, X. (2018). Carbon–nitrogen coupling under three schemes of model representation: a traceability analysis. *Geoscientific Model Development*, *11*(11), 4399–4416. https://doi.org/10.5194/gmd-11-4399-2018

Duan, A., & Wu, G. (2005). Role of the Tibetan Plateau thermal forcing in the summer climate patterns over subtropical Asia. *Climate Dynamics*, *24*(7-8), 793–807. https://doi.org/10.1007/s00382-004-0488-8

European Space Agency (2014) CCI land cover product user guide version 2.4, ESA CCI LC project.

Exbrayat, J. F., Pitman, A. J., & Abramowitz, G. (2014). Response of microbial decomposition to spin-up explains CMIP5 soil carbon range until 2100. *Geoscientific Model Development*, *7*, 2683–2692. https://doi.org/10.5194/gmd-7-2683-2014

Fang, X. (2011). Carbon exchange and its response to environmental factors in Poplar plantation ecosystem. Beijing Forestry University. Doctoral Dissertation.

Fatichi, S., Leuzinger, S., & Körner, C. (2014). Moving beyond photosynthesis: from carbon source to sink-driven vegetation modeling. *New Phytologist*, *201*(4), 1086–1095. https://doi.org/10.1111/nph.12614

Feng, G., Mi, X., Yan, H., Li, F. Y., Svenning, J. C., Ma, K., & Ecology, D. O. (2016). CForBio: a network monitoring Chinese forest biodiversity. *Science Bulletin*, *61*(15), 1163–1170. https://doi.org/10.1007/s11434-016-1132-9

Fernández-martínez, M. S., Vicca, I. A. J., Sardans, J., Luyssaert, S., Campioli, M., Chapin, F. S. III, et al. (2014). Nutrient availability as the key regulator of global forest carbon balance. *Nature Climate Change*, *4*(6), 471–476. https://doi.org/10.1038/nclimate2177

Friend, A. D., Lucht, W., Rademacher, T. T., Keribin, R., Betts, R., Cadule, P., et al. (2014). Carbon residence time dominates uncertainty in terrestrial vegetation responses to future climate and atmospheric CO_2. *Proceedings of the National Academy of Sciences of the United States of America*, *111*(9), 3280–3285. https://doi.org/10.1073/pnas.1222477110

org/10.1029/2010JG001566). The MOD15A2-LAI is acquired from ftp://ladsweb.nascom.nasa.gov website, and the GIMMS3g-LAI data set can be obtained from Boston University FTP site (ftp://crsftp.bu.edu/cliveg/). The aboveground biomass carbon (ABC) data set derived and used in this study can be accessed at http://www.wenfo.org/wald/global-biomass. The global forest age dataset (GFADv1.0), link to NetCDF file. *NASA National Aeronautics and Space Administration, PANGAEA*, https://doi.org/10.1594/PANGAEA.889943. The plant biomass dataset (consists of root, leaf and stem biomass, and stand age) can be obtained from Luo et al., 2014; doi:10.1016/j.forec-o.2012.01.005) and Zhang et al., 2015; doi:10.1088/1748-9326/10/4/044014). The observed vegetation C turnover time were derived from the database developed by Wang, Sun, et al., 2017; doi.org/10.1111/1365-2435.12914).

Fu, Z., Niu, S., & Dukes, J. S. (2015). What have we learned from global change manipulative experiments in China? A meta-analysis. *Scientific Reports*, *5*, 12344. https://doi.org/10.1038/srep12344

Geng, S. (2011). Study on the carbon flux observation over poplar plantation ecosystem of Xiping city in Hanan province of China. Beijing Forestry University. Master Dissertation.

Grömping, U. (2007). Estimators of relative importance in linear regression based on variance decomposition. *The American Statistician*, *61*(2), 139–147. https://doi.org/10.1198/000313007X188252

Guo, F., Liu, S., Wen, Y., Tang, J., Cai, D., Ming, A., & Shi, Z. (2015). Photosynthetic characteristics of eleven precious broadleaved tree species in south subtropics (in Chinese with english abstract). *Guangxi Sciencces*, *22*(6), 606–611. http://www.cnki.net/kcms/detail/45.1206.G3.20160106.1010.004.html

Guo, H. (2010). Carbon fluxes over an estuarine wetland: in situ measurement and modeling. Fudan University. Doctoral Dissertation.

Guo, Y., Wang, B., Xiang, W., Ding, T., Lu, S., Huang, F., et al. (2015). Density-dependent effects of tree species in a 15 ha seasonal rain forest plot in northern tropical karst in Nonggang, Guangxi, southern China. *Chinese Science Bulletin*, *60*(17), 1602–1611. https://doi.org/10.1360/N972014-00892

Han, S. (2008). Productivity estimation of the poplar plantations on the beaches in middle and low reaches of Yangtze river using eddy covariance measurement. Chinese Academy of Forestry. Doctoral Dissertation.

Hau, B. C. H., Dudgeon, D., & Corlett, R. T. (2005). Beyond Singapore: Hong Kong and Asian biodiversity. *Trends in Ecology & Evolution*, *20*(6), 281–282. https://doi.org/10.1016/j.tree.2005.04.002

Hayes, D. J., Mcguire, A. D., Kicklighter, D. W., Gurney, K. R., Burnside, T. J., & Melillo, J. M. (2011). Is the northern high-latitude land-based CO_2 sink weakening? *Global Biogeochemical Cycles*, *25*, GB3018. https://doi.org/10.1029/2010GB003813

He, H., Liu, M., Sun, X., Zhang, L., Luo, Y., Wang, H., et al. (2010). Uncertainty analysis of eddy flux measurements in typical ecosystems of ChinaFLUX. *Ecological Informatics*, *5*(6), 492–502. https://doi.org/10.1016/j.ecoinf.2010.07.004

Heimann, M., & Reichstein, M. (2008). Terrestrial ecosystem carbon dynamics and climate feedbacks. *Nature*, *451*, 289–292. https://doi.org/10.1038/nature06591

Hirata, R., Saigusa, N., Yamamoto, S., Ohtani, Y., Ide, R., Asanuma, J., et al. (2008). Spatial distribution of carbon balance in forest ecosystems across East Asia. *Agricultural and Forest Meteorology*, *148*(5), 761–775. https://doi.org/10.1016/j.agrformet.2007.11.016

Huang, H., Zhang, J. S., Meng, P., Fu, Y. L., Zheng, N., & Gao, J. (2011). Seasonal variation and meteorological control of CO_2 flux in a Hilly Plantation in the Mountain Areas of North China. *Acta Meteorologica Sinica*, *25*(2), 238–248. https://doi.org/10.1007/s13351-011-0030-y

Huang, S., Arain, M. A., Arora, V. K., Yuan, F., Brodeur, J., & Peichl, M. (2011). Analysis of nitrogen controls on carbon and water exchanges in a conifer forest using the CLASS-CTEM^{N+} model. *Ecological Modelling*, *222*(20-22), 3743–3760. https://doi.org/10.1016/j.ecolmodel.2011.09.008

Huntzinger, D. N., Michalak, A. M., Schwalm, C., Ciais, P., King, A. W., Fang, Y., et al. (2017). Uncertainty in the response of terrestrial carbon sink to environmental drivers undermines carbon-climate feedback predictions. *Scientific Reports*, *7*(1), 4765. https://doi.org/10.1038/s41598-017-03818-2

Huntzinger, D. N., Schwalm, C., Michalak, A. M., Schaefer, K., King, A. W., Wei, Y., et al. (2013). The North American carbon program Multi-Scale Synthesis and Terrestrial Model Intercomparison Project-Part 1: Overview and experimental design. *Geoscientific Model Development*, *6*(6), 2121–2133. https://doi.org/10.5194/gmd-6-2121-2013

Huntzinger, D. N., Schwalm, C., Wei, Y., Cook, R. B., Michalak, A. M., Schaefer, K., et al. (2018). NACP MsTMIP: Global 0.5-degree Model Outputs in Standard Format, Version 1.0. ORNL DAAC, Oak Ridge, Tennessee, USA. https://doi.org/10.3334/ORNLDAAC/1225

Ichii, K., Kondo, M., Lee, Y. H., Wang, S. Q., Kim, J., Ueyama, M., et al. (2013). Site-level model–data synthesis of terrestrial carbon fluxes in the CarboEastAsia eddy-covariance observation network: toward future modeling efforts. *Journal of Forest Research*, *18*(1), 13–20. https://doi.org/10.1007/s10310-012-0367-9

Iida, Y., Kohyama, T. S., Swenson, N. G., Su, S. H., Chen, C. T., Chiang, J. M., & Sun, I. F. (2014). Linking functional traits and demographic rates in a subtropical tree community: the importance of size dependency. *Journal of Ecology*, *102*(3), 641–650. https://doi.org/10.1111/1365-2745.12221

Intergovernmental Panel on Climate Change (2013). Summary for policymakers. In T. Stocker, D. Qin, & G. K. Plattner (Eds.), *Climate change 2013: The physical science basis. Contribution of Working Group I to the Fifth Assessment Report of the Intergovernmental Panel on Climate Change* (pp. 1–30). Cambridge, United Kingdom and New York, NY, USA: Cambridge University Press book section SPM.

Ito, A. (2010). Changing ecophysiological processes and carbon budget in East Asian ecosystems under near-future changes in climate: Implications for long-term monitoring from a process-based model. *Journal of Plant Research*, *123*(4), 577–588. https://doi.org/10.1007/s10265-009-0305-x

Ito, A., Inatomi, M., Huntzinger, D. N., Schwalm, C., Michalak, A. M., Cook, R., et al. (2016). Decadal trends in the seasonal-cycle amplitude of terrestrial CO_2 exchange resulting from the ensemble of terrestrial biosphere models. *Tellus Series B-chemical & Physical Meteorology*, *68*(1), 28968. https://doi.org/10.3402/tellusb.v68.28968

Ito, A., Inatomi, M., Mo, W., Lee, M., Koizumi, H., Saigusa, N., et al. (2007). Examination of model-estimated ecosystem respiration using flux measurements from a cool-temperate deciduous broad-leaved forest in central Japan. *Tellus. Series B: Chemical and Physical Meteorology*, *59*(3), 616–624. https://doi.org/10.1111/j.1600-0889.2007.00258.x

Ito, A., Nishina, K., Reyer, C. P. O., François, L., Henrot, A. J., Munhoven, G., et al. (2017). Photosynthetic productivity and its efficiencies in ISIMIP2a biome models: benchmarking for impact assessment studies. *Environmental Research Letters*, *12*. https://doi.org/10.1088/1748-9326/aa7a19

Jain, A., Yang, X., Haroon, K., David, M. G. A., Wilfred, P., & David, K. (2009). Nitrogen attenuation of terrestrial carbon cycle response to global environmental factors. *Global Biogeochemical Cycles*, *23*, GB4028. https://doi.org/10.1029/2009GB003519

Jiang, C., Ryu, Y., Fang, H., Myneni, R., Claverie, M., & Zhu, Z. (2017). Inconsistencies of interannual variability and trends in long-term satellite leaf area index products. *Global Change Biology*, *23*(10), 4133–4146. https://doi.org/10.1111/gcb.13787

Jung, M., Reichstein, M., Margolis, H. A., Cescatti, A., Richardson, A. D., Arain, M. A., et al. (2011). Global patterns of land-atmosphere fluxes of carbon dioxide, latent heat, and sensible heat derived from eddy covariance, satellite, and meteorological observations. *Journal of Geophysical Research*, *116*, G00J07. https://doi.org/10.1029/2010JG001566

Kato, T., Tang, Y., Gu, S., Hirota, M., Du, M., Li, Y., & Zhao, X. (2006). Temperature and biomass influences on interannual changes in CO_2 exchange in an alpine meadow on the Qinghai-Tibetan Plateau. *Global Change Biology*, *12*(7), 1285–1298. https://doi.org/10.1111/j.1365-2486.2006.01153.x

Kosugi, Y., Tanaka, H., Takanashi, S., Matsuo, N., Ohte, N., Shibata, S., & Tani, M. (2005). Three years of carbon and energy fluxes from Japanese evergreen broad-leaved forest. *Agricultural and Forest Meteorology*, *132*(3-4), 329–343. https://doi.org/10.1016/j.agrformet.2005.08.010

Krinner, G., Viovy, N., de Noblet-Ducoudré, N., Ogée, J., Polcher, J., Friedlingstein, P., et al. (2005). A dynamic global vegetation model for studies of the coupled atmosphere-biosphere system. *Global Biogeochemical Cycles*, *19*, GB1015. https://doi.org/10.1029/2003GB002199

Kröber, W., Böhnke, M., Welk, E., Wirth, C., Bruelheide, H., & Graae, B. J. (2012). Leaf trait-environment relationships in a subtropical broadleaved forest in South-East China. *PLoS ONE*, *7*(4). https://doi.org/10.1371/journal.pone.0035742

Kunstler, G., Falster, D., Coomes, D. A., Hui, F., Kooyman, R. M., Laughlin, D. C., et al. (2016). Plant functional traits have globally consistent effects on competition. *Nature*, *529*(7585), 204–207. https://doi.org/10.1038/nature16476

Kwon, H., Kim, J., Hong, J., & Lim, J. H. (2010). Influence of the Asian monsoon on net ecosystem carbon exchange in two major ecosystems in Korea. *Biogeosciences*, *7*(5), 1493–1504. https://doi.org/10.5194/bg-7-1493-2010

Lal, R. (2004). Soil carbon sequestration impacts on global climate change and food security. *Science*, *304*(5677), 1623–1627. https://doi.org/10.1126/science.1097396

Lan, G., Zhu, H., Cao, M., Hu, Y., Wang, H., Deng, X., et al. (2009). Spatial dispersion patterns of trees in a tropical rainforest in Xishuangbanna, southwest China. *Ecological Research*, *24*(5), 1117–1124. https://doi.org/10.1007/s11284-009-0590-9

Le, L., Mccormack, M. L., Ma, C., Kong, D., & Guo, D. (2015). Leaf economics and hydraulic traits are decoupled in five species-rich tropical-subtropical forests. *Ecology Letters*, *18*(9), 899–906. https://doi.org/10.1111/ele.12466

Lei, H., & Yang, D. (2010a). Seasonal and interannual variations in carbon dioxide exchange over a cropland in the North China Plain. *Global Change Biology*, *16*(11), 2944–2957. https://doi.org/10.1111/j.1365-2486.2009.02136.x

Lei, H., & Yang, D. (2010b). Interannual and seasonal variability in evapotranspiration and energy partitioning over an irrigated cropland in the North China Plain. *Agricultural and Forest Meteorology*, *150*(4), 581–589. https://doi.org/10.1016/j.agrformet.2010.01.022

Li, H., Huang, M., Wigmosta, M. S., Ke, Y., Coleman, A. M., Leung, R. L., et al. (2011). Evaluating runoff simulations from the community land model 4.0 using observations from flux towers and a mountainous watershed. *Journal of Geophysical Research*, *116*, D24120. https://doi.org/10.1029/2011JD016276

Li, Y., Zhang, C., Wang, N., Han, Q., Zhang, X., Liu, Y., et al. (2017). Substantial inorganic carbon sink in closed drainage basins globally. *Nature Geoscience*, *10*(7), 501–506. https://doi.org/10.1038/ngeo2972

Lindeman, R. H., Merenda, P. F., & Gold, R. Z. (1980). *Introduction to bivariate and multivariate analysis*. Scott, Foresman & Company Glenview, IL.

Liu, Y. Y., Dijk, A. I. J. M. V., Jeu, R. A. M. D., Canadell, J. G., Mccabe, M. F., Evans, J. P., & Wang, G. (2015). Recent reversal in loss of global terrestrial biomass. *Nature Climate Change*, *5*, 470–474. https://doi.org/10.1038/nclimate2581

Lu, Z. J., Bao, D. C., Guo, Y. L., Lu, J. M., Wang, Q. G., He, D., et al. (2013). Community composition and structure of Badagongshan (BDGS) forest dynamic plot in a mid-subtropical mountain evergreen and deciduous broad-leaved forest, central China (in Chinese with English abstract). *Plant Science Journal*, *31*(4), 336–344. https://doi.org/10.3724/SP.J.1142.2013.40336

Luo, L., Shen, G., Xie, Z., & Yu, J. (2011). Leaf functional traits of four typical forests along the altitudinal gradients in Mt Shennongjia. *Acta Ecologica Sinica*, *31*(21), 6420–6428. https://doi.org/10.1093/mp/ssq070

Luo, Y., Melillo, J., Niu, S., Beier, C., Clark, J. S., Classen, A. T., et al. (2011). Coordinated approaches to quantify long-term ecosystem dynamics in response to global change. *Global Change Biology*, *17*(2), 843–854. https://doi.org/10.1111/j.1365-2486.2010.02265.x

Luo, Y., Zhang, X., Wang, X., & Lu, F. (2014). Biomass and its allocation of Chinese forest ecosystems. *Ecology*, *95*(7), 2026–2026. https://doi.org/10.1890/13-2089.1

Mao, J., Thornton, P. E., Shi, X., Zhao, M., & Post, W. M. (2012). Remote Sensing Evaluation of CLM4 GPP for the Period 2000-09*. *Journal of Climate*, *25*, 5327–5342. https://doi.org/10.1175/JCLI-D-11-00401.1

Mao, W., Li, Y., Zhao, X., Zhang, T., & Liu, X. (2015). Variations of Leaf Economic Spectrum of Eight Dominant Plant Species in Two Successional Stages Under Contrasting Nutrient Supply. *Polish Journal of Ecology*, *64*(1), 14–24. https://doi.org/10.3161/15052249PJE2016.64.1.002

Medlyn, B. E., Zaehle, S., de Kauwe, M. G., Walker, A. P., Dietze, M. C., Hanson, P. J., et al. (2015). Using ecosystem experiments to improve vegetation models. *Nature Climate Change*, *5*(6), 528–534. https://doi.org/10.1038/nclimate2621

Musavi, T., Mahecha, M. D., Migliavacca, M., Reichstein, M., van de Weg, M. J., van Bodegom, P. M., et al. (2015). The imprint of plants on ecosystem functioning: a data-driven approach. *International Journal of Applied Earth Observation & Geoinformation*, *43*, 119–131. https://doi.org/10.1016/j.jag.2015.05.009

Musavi, T., Migliavacca, M., Reichstein, M., Kattge, J., Wirth, C., Black, T. A., et al. (2017). Stand age and species richness dampen interannual variation of ecosystem-level photosynthetic capacity. *Nature ecology & evolution*, *1*(2), 0048. https://doi.org/10.1038/s41559-016-0048

New, M., Lister, D., Hulme, M., & Makin, I. (2002). A high-resolution data set of surface climate over global land areas. *Climate Research*, *21*, 1–25. https://doi.org/10.3354/cr021001

Norby, R. J., de Kauwe, M. G., Domingues, T. F., Duursma, R. A., Ellsworth, D. S., Goll, D. S., et al. (2016). Model-data synthesis for the next generation of forest free-air CO_2 enrichment (FACE) experiments. *New Phytologist*, *209*(1), 17–28. https://doi.org/10.1111/nph.13593

Oleson, K. W., Lawrence, D. M., Bonan, G. B., Drewniak, B., Huang, M., Koven, C. D., et al. (2013). Technical description of version 4.5 of the Community Land Model (CLM). NCAR Technical Note. https://doi.org/10.5065/D6RR1W7M

Ono, K., Mano, M., Han, G. H., Nagai, H., Yamada, T., Kobayashi, Y., et al. (2013). Environmental controls on fallow carbon dioxide flux in a single-crop rice paddy, Japan. *Land Degradation & Development*, *26*(4), 331–339. https://doi.org/10.1002/ldr.2211

Peng, C., Zhu, Q., & Chen, H. (2013). Integrating greenhouse gas emission processes into a dynamic global vegetation model of TRIPLEX-GHG. Egu General Assembly Conference. EGU General Assembly Conference Abstracts. http://meetingorganizer.copernicus.org/EGU2013/EGU2013-1486.pdf

Peng, S., Ciais, P., Chevallier, F., Peylin, P., Cadule, P., Sitch, S., et al. (2015). Benchmarking the seasonal cycle of CO_2 fluxes simulated by terrestrial ecosystem models. *Global Biogeochemical Cycles*, *29*, 46–64. https://doi.org/10.1002/2014GB004931

Pfeifer, M., Lefebvre, V., Turner, E., Cusack, J., Khoo, M. S., Chey, V. K., et al. (2015). Deadwood biomass: an underestimated carbon stock in degraded tropical forests? *Environmental Research Letters*, *10*(4). https://doi.org/10.1088/1748-9326/10/4/044019

Poorter, H., Niklas, K. J., Reich, P. B., Oleksyn, J., Poot, P., & Mommer, L. (2012). Biomass allocation to leaves, stems and roots: meta-analyses of interspecific variation and environmental control. *New Phytologist*, *193*(1), 30–50. https://doi.org/10.1111/j.1469-8137.2011.03952.x

Poulter, B., Aragão, L., Andela, N., Bellassen, V., Ciais, P., Kato, T., et al. (2018). *The global forest age dataset (GFADv1.0)*. NASA National Aeronautics and Space Administration, *PANGAEA*. https://doi.org/10.1594/PANGAEA.889943

Poulter, B., Aragão, L., Heyder, U., Gumpenberger, M., Heinke, J., Langerwisch, F., et al. (2010). Net biome production of the amazon basin in the 21st century. *Global Change Biology*, *16*(7), 2062–2075. https://doi.org/10.1111/j.1365-2486.2009.02064.x

Qian, H., Joseph, R., & Zeng, N. (2010). Enhanced terrestrial carbon uptake in the Northern High Latitudes in the 21st century from the Coupled Carbon Cycle Climate Model Intercomparison Project model projections. *Global Change Biology*, *16*(2), 641–656. https://doi.org/10.1111/j.1365-2486.2009.01989.x

Qin, Y., Xiao, X., Dong, J., Zhang, G., Roy, P. S., Joshi, P. K., et al. (2016). Mapping forests in monsoon Asia with ALOS PALSAR 50-m mosaic images and MODIS imagery in 2010. *Scientific Reports*, *6*(1), 20880. https://doi.org/10.1038/srep20880

R Development Core Team, 2011. (2011). R Development Core Team R: A Language and Environment for Statistical Computing 3-900051-07-0, Assessment of model estimates of land-atmosphere CO_2 exchange across Northern Eurasia, Vienna, Austria. http://www.R-project.org/

Rawlins, M. A., McGuire, A. D., Kimball, J. S., Dass, P., Lawrence, D., Burke, E., et al. (2015). Assessment of model estimates of land-atmosphere CO_2 exchange across Northern Eurasia. *Biogeosciences*, *12*(14), 4385–4405. https://doi.org/10.5194/bg-12-4385-2015

Reich, P. B., Luo, Y., Bradford, J. B., Poorter, H., Perry, C. H., & Oleksyn, J. (2014). Temperature drives global patterns in forest biomass distribution in leaves, stems, and roots. *Proceedings of the National Academy of Sciences*, *111*(38), 13,721–13,726. https://doi.org/10.1073/pnas.1216053111

Reichstein, M., Bahn, M., Mahecha, M. D., Kattge, J., & Baldocchi, D. D. (2014). Linking plant and ecosystem functional biogeography. *Proceedings of the National Academy of Sciences of the United States of America*, *111*(38), 13,697–13,702. https://doi.org/10.1073/pnas.1216065111

Rogers, A., Medlyn, B. E., Dukes, J. S., Bonan, G., von Caemmerer, S., Dietze, M. C., et al. (2017). A roadmap for improving the representation of photosynthesis in Earth system models. *New Phytologist*, *213*(1), 22–42. https://doi.org/10.1111/nph.14283

Rollinson, C. R., Liu, Y., Raiho, A., Moore, D. J. P., McLachlan, J., Bishop, D. A., et al. (2017). Emergent climate and CO_2 sensitivities of net primary productivity in ecosystem models do not agree with empirical data in temperate forests of eastern North America. *Global Change Biology*, *23*(7), 2755–2767. https://doi.org/10.1111/gcb.13626

Running, S. W., Zhao, M. (2015). User's guide: Daily GPP and annual NPP (MOD17A2/A3) products NASA Earth Observing System MODIS land algorithm.

Saatchi, S. S., & Morel, A. (2011). Benchmark map of forest carbon stocks in tropical regions across three continents. *Proceedings of the National Academy of Sciences of the United States of America*, *108*(24), 9899–9904. https://doi.org/10.1073/pnas.1019576108

Saigusa, N., Yamamoto, S., Murayama, S., & Kondo, H. (2005). Inter-annual variability of carbon budget components in an AsiaFlux forest site estimated by long-term flux measurements. *Agricultural and Forest Meteorology*, *134*(1-4), 4–16. https://doi.org/10.1016/j.agrformet.2005.08.016

Saito, M., Miyata, A., Nagai, H., & Yamada, T. (2006). Seasonal variation of carbon dioxide exchange in rice paddy field in Japan. *Agricultural and Forest Meteorology*, *135*(1-4), 93–109. https://doi.org/10.1016/j.agrformet.2005.10.007

Saitoh, T. M., Tamagawa, I., Muraoka, H., Lee, N. Y. M., Yashiro, Y., & Koizumi, H. (2010). Carbon dioxide exchange in a cool-temperate evergreen coniferous forest over complex topography in Japan during two years with contrasting climates. *Journal of Plant Research*, *123*(4), 473–483. https://doi.org/10.1007/s10265-009-0308-7

Sakschewski, B., von Bloh, W., Boit, A., Rammig, A., Kattge, J., Poorter, L., et al. (2015). Leaf and stem economics spectra drive diversity of functional plant traits in a dynamic global vegetation model. *Global Change Biology*, *21*(7), 2711–2725. https://doi.org/10.1111/gcb.12870

Schaefer, K., Schwalm, C. R., Williams, C., Arain, M. A., Barr, A., Chen, J. M., et al. (2012). A model-data comparison of gross primary productivity: Results from the North American Carbon Program site synthesis. *Journal of Geophysical Research*, *117*, G03010. https://doi.org/10.1029/2012JG001960

Schaefer, K., Zhang, T., Slater, A. G., Lu, L., Etringer, A., & Baker, I. (2009). Improving simulated soil temperatures and soil freeze/thaw at high-latitude regions in the Simple Biosphere/Carnegie-Ames-Stanford Approach model. *Journal of Geophysical Research*, *114*, F02021. https://doi.org/10.1029/2008JF001125

Schwalm, C. R., Huntzinger, D. N., Fisher, J. B., Michalak, A. M., Bowman, K., Ciais, P., et al. (2015). Toward "optimal" integration of terrestrial biosphere models. *Geophysical Research Letters*, *42*, 4418–4428. https://doi.org/10.1002/2015GL064002

Schwalm, C. R., Williams, C. A., Schaefer, K., Anderson, R., Arain, M. A., Baker, I., et al. (2010). A model-data intercomparison of CO_2 exchange across North America: Results from the North American Carbon Program site synthesis. *Journal of Geophysical Research*, *115*, G00H05. https://doi.org/10.1029/2009JG001229

Shimoda, S., Mo, W., & Oikawa, T. (2005). The effects of characteristics of Asian Monsoon Climate on interannual CO_2 exchange in a humid temperate C3/C4 co-occurring grassland. *Sola*, *1*, 169–172. https://doi.org/10.2151/sola.2005-044

Sitch, S., Smith, B., Prentice, I. C., Arneth, A., & Venevsky, S. (2003). Evaluation of ecosystem dynamics, plant geography and terrestrial carbon cycling in the LPJ dynamic global vegetation model. *Global Change Biology*, *9*(2), 161–185. https://doi.org/10.1046/j.1365-2486.2003.00569.x

Smith, W. K., Reed, S. C., Cleveland, C. C., Ballantyne, A. P., Anderegg, W. R. L., Wieder, W. R., et al. (2015). Large divergence of satellite and Earth system model estimates of global terrestrial CO_2 fertilization. *Nature Climate Change*, *6*(3), 306–310. https://doi.org/10.1038/nclimate2879

Song, Y., Yan, E., & Song, K. (2015). Synthetic comparison of eight dynamics plots in evergreen broadleaf forests, China. *Biodiversity Science*, *23*(2), 139–148. https://doi.org/10.17520/biods.2014140

Strengbom, J., & Reich, P. B. (2006). Elevated [CO] and Increased N Supply Reduce Leaf Disease and Related Photosynthetic Impacts on Solidago rigida. *Oecologia*, *149*(3), 519–525. https://doi.org/10.1007/s00442-006-0458-4

Su, S., Chang-Yang, C., Lu, C., Tsui, C., Lin, T., Lin, C., et al. (2007). *Fushan Subtropical Forest Dynamics Plot: Tree Species Characteristics and Distribution Patterns (in Chinese with English abstract)*. Taipei: Taiwan Forestry Research Institute. http://ntur.lib.ntu.edu.tw/handle/246246/201637

Sun, J. (2012). Study of CO2 flux above urban green space in Perl River Delta. Nanjing University of Information Science and Technology. Master Dissertation.

Swenson, N. G., & Weiser, M. D. (2010). Plant geography upon the basis of functional traits: an example from eastern North American trees. *Ecology*, *91*(8), 2234–2241. https://doi.org/10.1890/09-1743.1

Takanashi, S., Kosugi, Y., Tanaka, Y., Yano, M., Katayama, T., Tanaka, H., & Tani, M. (2005). CO_2 exchange in a temperate Japanese cypress forest compared with that in a cool-temperate deciduous broad-leaved forest. *Ecological Research*, *20*(3), 313–324. https://doi.org/10.1007/s11284-005-0047-8

Tan, Z., Zhang, Y., Schaefer, D., Yu, G., Liang, N., & Song, Q. (2011). An old-growth subtropical Asian evergreen forest as a large carbon sink. *Atmospheric Environment*, *45*(8), 1548–1554. https://doi.org/10.1016/j.atmosenv.2010.12.041

Tan, Z. H., Zhang, Y. P., Liang, N., Hsia, Y. J., Zhang, Y. J., Zhou, G. Y., et al. (2012). An observational study of the carbon-sink strength of East Asian subtropical evergreen forests. *Environmental Research Letters*, *7*(4). https://doi.org/10.1088/1748-9326/7/4/044017

Taylor, K. E. (2001). Summarizing multiple aspects of model performance in a single diagram. *Journal of Geophysical Research*, *106*(D7), 7183–7192. https://doi.org/10.1029/2000JD900719

Thornton, P. E., Law, B. E., Gholz, H. L., Clark, K. L., Falge, E., Ellsworth, D. S., et al. (2002). Modeling and measuring the effects of disturbance history and climate on carbon and water budgets in evergreen needleleaf forests. *Agricultural & Forest Meteorology*, *113*(1-4), 185–222. https://doi.org/10.1016/S0168-1923(02)00108-9

Thurner, M., Beer, C., Ciais, P., Friend, A. D., Ito, A., Kleidon, A., et al. (2017). Evaluation of climate-related carbon turnover processes in global vegetation models for boreal and temperate forests. *Global Change Biology*, *23*(8), 3076–3091. https://doi.org/10.1111/gcb.13660

Tian, H., Melillo, J. M., Kicklighter, D. W., Pan, S., Liu, J., Mcguire, A. D., & Iii, B. M. (2003). Regional carbon dynamics in monsoon Asia and its implications for the global carbon cycle. *Global & Planetary Change*, *37*(3-4), 201–217. https://doi.org/10.1016/S0921-8181(02)00205-9

Tian, H., Xu, X., Lu, C., Liu, M., Ren, W., Chen, G., et al. (2011). Net exchanges of CO_2, CH_4, and N_2O between China's terrestrial ecosystems and the atmosphere and their contributions to global climate warming. *Journal of Geophysical Research*, *116*, G02011. https://doi.org/10.1029/2010JG001393

Tjiputra, J. F., Roelandt, C., Bentsen, M., Lawrence, D. M., Lorentzen, T., Schwinger, J., et al. (2013). Evaluation of the carbon cycle components in the Norwegian Earth System Model (NorESM). *Geoscientific Model Development*, *6*(2), 301–325. https://doi.org/10.5194/gmd-6-301-2013

Todd-Brown, K. E. O., Randerson, J. T., Hopkins, F., Arora, V., Hajima, T., Jones, C., et al. (2014). Changes in soil organic carbon storage predicted by Earth system models during the 21st century. *Biogeosciences*, *11*(8), 2341–2356. https://doi.org/10.5194/bg-11-2341-2014

Verheijen, L. M., Brovkin, V., Aerts, R., Bönisch, G., Cornelissen, J. H. C., Kattge, J., et al. (2013). Impacts of trait variation through observed trait-climate relationships on performance of an earth system model: a conceptual analysis. *Biogeosciences*, *10*(8), 5497–5515. https://doi.org/10.5194/bg-10-5497-2013

Walker, A. P., Quaife, T., van Bodegom, P. M., de Kauwe, M. G., Keenan, T. F., Joiner, J., et al. (2017). The impact of alternative trait-scaling hypotheses for the maximum photosynthetic carboxylation rate (V_{cmax}) on global gross primary production. *New Phytologist*, *215*(4), 1370–1386. https://doi.org/10.1111/nph.14623

Wang, D., Ricciuto, D., Post, W., & Berry, M. W. (2011). Terrestrial Ecosystem Carbon Modeling. *Encyclopedia of Parallel Computing*, 2034–2039. https://doi.org/10.1007/978-0-387-09766-4

Wang, J., Sun, J., Xia, J., He, N., Li, M., & Niu, S. (2017). Soil and vegetation carbon turnover times from tropical to boreal forests. *Functional Ecology*, *32*(1), 71–82. https://doi.org/10.1111/1365-2435.12914

Wang, R., Goll, D., Balkanski, Y., Hauglustaine, D., Boucher, O., Ciais, P., et al. (2017). Global forest carbon uptake due to nitrogen and phosphorus deposition from 1850 to 2100. *Global Change Biology*, *23*(11), 4854–4872. https://doi.org/10.1111/gcb.13766

Wang, Y., Tao, J., Liu, J., & He, Z. (2012). Response of leaf functional traits to different light regimes in an evergreen broad-leaved forest in the Jinyun Mountain. *Scientia Silvae Sinicae*, *6*(2), 288–293. https://doi.org/10.1007/s11783-011-0280-z

Wei, Y., Liu, S., Huntzinger, D. N., Michalak, A. M., Viovy, N., Post, W. M., et al. (2014a). NACP MsTMIP: Global and North American Driver Data for Multi-Model Intercomparison. ORNL DAAC, Oak Ridge, Tennessee, USA. https://doi.org/10.3334/ORNLDAAC/1220.

Wei, Y., Liu, S., Huntzinger, D. N., Michalak, A. M., Viovy, N., Post, W. M., et al. (2014b). The North American carbon program Multi-scale Synthesis and Terrestrial Model Intercomparison Project: Part 2- Environmental Driver Data. *Geoscientific Model Development*, *7*(6), 2875–2893. https://doi.org/10.5194/gmd-7-2875-2014

Wu, L., Gu, S., Zhao, L., Xu, S., Zhou, H., & Feng, C. (2010). Variation in net CO_2 exchange, gross primary production and its affecting factors in the planted pasture ecosystem in Sanjiangyuan Region of the Qinghai-Tibetan Plateau of China. *Chinese Journal of Plant Ecology*, *30*(4), 521–528. https://doi.org/10.3724/SP.J.1142.2010.40521

Wu, Z., Ahlstroem, A., Smith, B., Ardo, J., Eklundh, L., Fensholt, R., & Lehsten, V. (2017). Climate data induced uncertainty in model based estimations of terrestrial primary productivity. *Environmental Research Letters*, *12*(6). https://doi.org/10.1088/1748-9326/aa6fd8

Xia, J., McGuire, A. D., Lawrence, D., Burke, E., Chen, G., Chen, X., et al. (2017). Terrestrial ecosystem model performance in simulating productivity and its vulnerability to climate change in the northern permafrost region. *Journal of Geophysical Research: Biogeosciences*, *122*, 430–446. https://doi.org/10.1002/2016JG003384

Xia, J., Niu, S., Ciais, P., Janssens, I. A., Chen, J., Ammann, C., et al. (2015). Joint control of terrestrial gross primary productivity by plant phenology and physiology. *Proceedings of the National Academy of Sciences of the United States of America*, *112*(9), 2788–2793. https://doi.org/10.1073/pnas.1413090112

Xiao, Z., Liang, S., & Jiang, B. (2017). Evaluation of four long time-series global leaf area index products. *Agricultural & Forest Meteorology*, *246*, 218–230. https://doi.org/10.1016/j.agrformet.2017.06.016

Xu, M., Zhao, Y., Yang, X., Shi, Q., Zhou, L., Zhang, Q., et al. (2016). Geostatistical analysis of spatial variations in leaf traits of woody plants in Tiantong, Zhejiang province. *Chinese Journal of Plant Ecology*, *40*(01), 48–59. https://doi.org/10.17521/cjpe.2015.0246

Yan, K., Park, T., Yan, G., Chen, C., Yang, B., Liu, Z., et al. (2016). Evaluation of MODIS LAI/FPAR product collection 6. Part 1: Consistency and improvements. *Remote Sensing*, *8*(5). https://doi.org/10.3390/rs8050359

Yan, Y. (2009). Carbon flux in an enstuarine wetland estimated by remote model and groud-based observations. Fudan University. Doctoral Dissertation.

Yang, Q., Ma, Z., Xie, Y., Zhang, Z., Wang, Z., Liu, H., et al. (2011). Community structure and species composition of an evergreen broadleaved forest in Tiantong's 20 ha dynamic plot, Zhejiang Province, eastern China (in Chinese with English abstract). *Biodiversity Science*, *19*(2), 215–223. https://doi.org/10.3724/SP.J.1003.2011.09013

Yang, X., Yan, E., Chang, S., Da, L., & Wang, X. (2015). Tree architecture varies with forest succession in evergreen broad-leaved forests in Eastern China. *Trees*, *29*(1), 43–57. https://doi.org/10.1007/s00468-014-1054-6

Yang, Y., Zhu, Q., Peng, C., Wang, H., & Chen, H. (2015). From plant functional types to plant functional traits: A new paradigm in modelling global vegetation dynamics. *Progress in Physical Geography: Earth and Environment*, *39*(4), 514–535. https://doi.org/10.1177/0309133315582018

Yao, Y., Wang, X., Li, Y., Wang, T., Shen, M., Du, M., et al. (2017). Spatiotemporal pattern of gross primary productivity and its covariation with climate in China over the last thirty years. *Global Change Biology*, *24*(1), 184–196. https://doi.org/10.1111/gcb.13830

Yin, Q., Wang, L., Lei, M., Dang, H., Quan, J., Tian, T., et al. (2018). The relationships between leaf economics and hydraulic traits of woody plants depend on water availability. *Science of the Total Environment*, *621*, 245–252. https://doi.org/10.1016/j.scitotenv.2017.11.171

Yu, G., Chen, Z., Piao, S., Peng, C., Ciais, P., Wang, Q., et al. (2014). High carbon dioxide uptake by subtropical forest ecosystems in the East Asian monsoon region. *Proceedings of the National Academy of Sciences of the United States of America*, *111*(13), 4910–4915. https://doi.org/10.1073/pnas.1317065111

Yu, G. R., Zhu, X. J., Fu, Y. L., He, H. L., Wang, Q. F., Wen, X. F., et al. (2013). Spatial pattern and climate drivers of carbon fluxes in terrestrial ecosystems of China. *Global Change Biology*, *19*(3), 798–810. https://doi.org/10.1111/gcb.12079

Zeng, N., Mariotti, A., & Wetzel, P. (2005). Terrestrial mechanisms of interannual CO_2 variability. *Global Biogeochemical Cycles*, *19*, GB1016. https://doi.org/10.1029/2004GB002273

Zha, T. (2007). Carbon balance of a poplar plantation ecosystem in Daxing, Beijing. Beijing Forestry University. Doctoral Dissertation.

Zhang, H., Wang, K., Xu, X., Song, T., Xu, Y., & Zeng, F. (2015). Biogeographical patterns of biomass allocation in leaves, stems, and roots in China's forests. *Scientific Reports*, *5*, 15997. https://doi.org/10.1038/srep15997

Zhang, L. (2010). Characteristics of CO2 flux in a Chinese Fir plantations ecosystem in Huitong County, Human Province. Central South University of Forestry and Technology. Master Dissertation.

Zhang, R. (2015). Natural and human-induced changes in summer climate over the East Asian monsoon region in the last half century: A review. *Advances in Climate Change Research*, *6*(2), 131–140. https://doi.org/10.1016/j.accre.2015.09.009

Zhang, Y., Tan, Z., Song, Q., Yu, G., & Sun, X. (2010). Respiration controls the unexpected seasonal pattern of carbon flux in an Asian tropical rain forest. *Atmospheric Environment*, *44*(32), 3886–3893. https://doi.org/10.1016/j.atmosenv.2010.07.027

Zhao, Z. (2011). A study on carbon flux between Chinese fir planations and atmosphere in subtropical belts. Central South University of Forestry and Technology. Doctoral Dissertation.

Zhu, Q., Liu, J., Peng, C., Chen, H., Fang, X., Jiang, H., et al. (2014). Modelling methane emissions from natural wetlands by development and application of the TRIPLEX-GHG model. *Geoscientific Model Development*, *7*(3), 981–999. https://doi.org/10.5194/gmd-7-981-2014

Zhu, Y. (2005). Carbon dioxide exchange between paddy ecosystem and the atmosphere in the subtropical region. Chinese Academy of Sciences and Ministry of Education. Doctoral Dissertation.

Zhu, Z., Bi, J., Pan, Y., Ganguly, S., Anav, A., Xu, L., et al. (2013). Global data sets of vegetation leaf area index (LAI)3g and fraction of photosynthetically active radiation (FPAR)3g derived from global inventory modeling and mapping studies (GIMMS) normalized difference vegetation index (NDVI3g) for the period 1981 to 2011. *Remote Sensing*, *5*(2), 927–948. https://doi.org/10.3390/rs5020927

Zhu, Z., Piao, S., Lian, X., Myneni, R. B., Peng, S., & Yang, H. (2017). Attribution of seasonal leaf area index trends in the northern latitudes with "optimally" integrated ecosystem models. *Global Change Biology*, *23*(11), 4798–4813. https://doi.org/10.1111/gcb.13723

Zhu, Z., Piao, S., Myneni, R. B., Huang, M., Zeng, Z., Canadell, J. G., et al. (2016). Greening of the Earth and its drivers. *Nature Climate Change*, *6*(8), 791–795. https://doi.org/10.1038/nclimate3004